International Journal of Pharmaceutics 635 (2023) 122722

Contents lists available at ScienceDirect

International Journal of Pharmaceutics

journal homepage: www.elsevier.com/locate/ijpharm

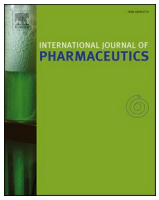

# Enhanced blend uniformity and flowability of low drug loaded fine API blends via dry coating: The effect of mixing time and excipient size

Sangah S. Kim, Chelsea Castillo, Mirna Cheikhali, Hadeel Darweesh, Christopher Kossor, Rajesh N. Davé *

*New Jersey Center for Engineered Particulates, New Jersey Institute of Technology, Newark, NJ 07102, USA*

ARTICLE INFO

*Keywords:*
Dry coating
Blend uniformity
Excipient size
Blend flowability
Agglomeration

ABSTRACT

Although previous research demonstrated improved flowability, packing, fluidization, etc. of individual powders via nanoparticle dry coating, none considered its impact on very low drug loaded blends. Here, fine ibuprofen at 1, 3, and 5 wt% drug loadings (DL) was used in multi-component blends to examine the impact of the excipients size, dry coating with hydrophilic or hydrophobic silica, and mixing times on the blend uniformity, flowability and drug release rates. For uncoated active pharmaceutical ingredients (API), the blend uniformity (BU) was poor for all blends regardless of the excipient size and mixing time. In contrast, for dry coated API having low agglomerate ratio (AR), BU was dramatically improved, more so for the fine excipient blends, at lesser mixing times. For dry coated API, the fine excipient blends mixed for 30 min had enhanced flowability and lower AR; better for the lowest DL having lesser silica, likely due to mixing induced synergy of silica redistribution. For the fine excipient tablets, dry coating led to fast API release rates even with hydrophobic silica coating. Remarkably, the low AR of the dry coated API even at very low DL and amounts of silica in the blend led to the enhanced blend uniformity, flow, and API release rate.

## 1. Introduction

Powder mixing is an active area of research where both industry and academia have investigated the influence of physicochemical properties of powders and processing conditions on mixture uniformity (Bridgwater, 2012; Carson et al., 1986; Poux et al., 1991; Rohrs et al., 2006; Tang and Puri, 2004). For example, particle size, particle size distribution (PSD) and its span, and the dosage of an active ingredient have been identified to have a significant impact to achieve the USP recommended stage 1 uniformity (Poux et al., 1991; Rohrs et al., 2006). Unfortunately, the complexity of powder behavior including their cohesion and tendency to agglomerate (Kendall, 1994; Rumpf, 1974; Tinke et al., 2009), indicates that selecting a proper fine size for a given dose cannot assure mixture uniformity. Thus, active pharmaceutical ingredient (API) powder agglomeration and the mixing process significantly impact blend uniformity (BU) for finer API at low drug loading (Huang et al., 2017; Rohrs et al., 2006; Zheng, 2008). In fact, a recent review paper discussing the blend uniformity and segregation issues encountered in the tablet manufacturing process (Jakubowska and Ciepluch, 2021) highlights the difficulties in achieving uniform powder blends for the cohesive, poorly flowing API powders. The authors emphasized that such problems cannot be solved by focusing on the processing equipment or operating parameters alone and mitigation of powder cohesion is necessary. Likewise, others have recognized such issues; e.g., the dependence of the material properties (coarse and non-cohesive excipients) (Alyami et al., 2017), the standard operating procedure identifying the time to add additives like magnesium stearate (Muselík et al., 2014), and the selection of the blending equipment and processing time (Alyami et al., 2017). Nonetheless, such approaches have not been able to address the fundamental problem of high cohesion and ensuing agglomeration of fine API powders.

The problem of high cohesion has been successfully addressed through solventless dry coating approach, where smaller guest particles are attached mechanically onto larger host particle surfaces leading to significantly reduced fine micronized API powder cohesion (Chen et al., 2018a, 2008; Naito et al., 2003; Pfeffer et al., 2001; Yang et al., 2005; Yokoyama et al., 1987). Resulting reduced particle cohesion helps alleviate problems in powder handling and product quality in

* Corresponding author. Address: Distinguished Professor of Chemical and Materials Engineering, New Jersey Center for Engineered Particulates, New Jersey Institute of Technology, Newark, NJ 07102, USA.
*E-mail address:* dave@njit.edu (R.N. Davé).

https://doi.org/10.1016/j.ijpharm.2023.122722
Received 29 October 2022; Received in revised form 8 February 2023; Accepted 9 February 2023
Available online 14 February 2023

pharmaceutical industry. Numerous research groups have examined dry coating of individual powders using various nanoparticles, e.g., metal oxides such as fumed silica, titania, alumina, etc. (Gera et al., 2010; Honda et al., 1988, 1989; Honda et al., 1987; Iwasaki, 2011; Kujawa et al., 2014; Meyer and Zimmermann, 2004; Ouabbas et al., 2009; Watano et al., 2000; Zhang et al., 2009; Zhu et al., 2005; Zimmermann et al., 2004) or spreadable materials, e.g., magnesium stearate (MgSt), leucine, etc. (Brunaugh and Smyth, 2018; Koskela et al., 2018; Li et al., 2016; Pingali et al., 2011; Qu et al., 2015a 2015b; Sierra-Vega et al., 2019; Zhou et al., 2011). Typically, dry coating requires use of higher intensity mixing devices instead of conventional mixers. Examples include Japanese devices such as mechanofusion (Koishi et al., 1987, 1984; Naito et al., 2003; Tanno, 1990; Yokoyama et al., 1987), hybridizer (Ishizaka et al., 1988; Senna, 1998, 1999), and theta-composer (Alonso, 1991; Kawashima et al., 1998; Suzuki et al., 1997; Watano et al., 2000), which have been introduced over three decades ago. Likewise, an innovative device called the Magnetically Assisted Impaction Coating (MAIC) was introduced in the USA over two decades ago (Hendrickson and Kooyer, 2000), whereas our group has been involved with proposing four novel approaches, the rotating fluidized bed coater (Watano et al., 2001), simultaneous milling and coating (Zhang et al., 2009), conical mill (Mullarney et al., 2011a), and a high-intensity vibratory coater (Mullarney et al., 2011b). The Japanese devices, the MAIC, as well as those introduced and promoted by our group have also been used by others; for example, mechanofusion (Koskela et al., 2018), the conical mill based coating (Capece et al., 2021; Chattoraj et al., 2011), simultaneous milling and coating (Liu et al., 2012; Wang et al., 2009), and high-intensity vibratory mixer (Kottlan et al., 2023; Osorio and Muzzio, 2015).

Such reports have demonstrated resulting improved bulk powder properties such as flowability (Chen et al., 2018b; Jallo et al., 2012; Mei et al., 1997; Ono and Yonemochi, 2020; Qu et al., 2015a; Xu et al., 2009; Zhou et al., 2011), packing density (Chen et al., 2022, 2019; Fu et al., 2006; Jallo et al., 2012; Mullarney et al., 2011a; Valverde and Castellanos, 2007; Yano et al., 2021), fluidization (Chen et al., 2008; Xu et al., 2009; Zhou and Zhu, 2019, 2021), and dissolution (Han et al., 2013a; Ishizaka et al., 1993; Qu et al., 2015b; Saeki et al., 2019). In addition, has been shown to significantly reduce fine micronized powder cohesion and subsequent agglomeration (Han et al., 2011; Huang et al., 2017; Kim et al., 2021; Qu et al., 2015a, 2015b; Shah et al., 2017; Sharma and Setia, 2019).

A large body of work has also examined dispersibility of powders and inhalation formulations, and demonstrated improved powder aerosolization, stability, and absorption rate by modifying the surface properties of the low-micron API particles (Adi et al., 2013; Jetzer et al., 2018; Kaialy and Nokhodchi, 2015; Kunnath et al., 2021; Paajanen et al., 2009; Park et al., 2021; Qu et al., 2015a; Shetty et al., 2020; Tan et al., 2016; Xu et al., 2009; Zhou et al., 2015, 2011; Zhou and Zhu, 2019, 2021; Zijlstra et al., 2004). However, this body of work did not consider industry relevant multi-component blend formulations intended for tablets, capsules and sachet blends, in particular those suitable for direct compression tableting. Such blends, especially when the API is cohesive and the drug loading is low, the subject of this work, are different in several aspects and pose different types of challenges. For example, oral dosage formulations pose specific challenges for both low (<5 wt%) and high (>25 wt%) drug loadings; in the former, difficulty in attaining blend uniformity (BU) and API content uniformity (CU), and in the latter, attaining adequate flowability, tablet weight variability and dissolution (Engisch and Muzzio, 2015; Mehrotra, 2010; Sacher et al., 2020; Schaller et al., 2019). Unlike inhalation formulations, tablet and capsule formulations must include multitude of functional excipients that must be well-mixed in a blend. At the same time, those formulations can use nano-silica in contrast to inhalation formulations that cannot, yet the amount of added silica must be capped at 2 wt% (FDA, 2022). For example, ideal oral tablet blend should have adequate flowability and bulk density, lack of unwanted API agglomeration, good blend uniformity, very low drug segregation tendency during processing steps, good compressibility and tableting properties, desired drug dissolution, and preferably, be suitable for direct blending and direct compression (DB-DC) tableting process. That is because if the blend is not BD-DC capable, the use of solvent in multiple steps may be necessary, leading to higher cost of manufacturing and higher environmental footprint and making conversion from batch to continuous more difficult (Lee et al., 2015; Schaber et al., 2011).

Towards the objective of making the blends BD-DC capable while having reduced environmental footprint, solventless mechanical dry coating approach has become increasingly popular in developing better oral solid dosage formulations. For example, several reports have demonstrated the impact of dry coating of a single constituent of the blend on enhanced tablet properties (Chen et al., 2019; Huang et al., 2015b; Kunnath et al., 2018), enhanced dissolution for hydrophilic silica coated ibuprofen (Han et al., 2013a), and reduced agglomeration of micronized API after dry coating hydrophobic silica on improving the content uniformity of blends (Huang et al., 2017; Kim et al., 2022b). Huang et al. 2017 demonstrated significantly improved a binary powder BU of 3, 5, and 10 wt% fine micronized acetaminophen (mAPAP) after dry coating mAPAP with silica (Huang et al., 2017), showing no need for additional granulation or mixing steps to achieve targeted FFC and BU thereby enabling DB-DC. More recently, (Kim et al., 2022b) demonstrated that even for finer excipients, the BU of fine micronized ibuprofen (Ibu), a poorly water-soluble drug, could be significantly enhanced at even lower, 1, 3, and 5 wt% of dry coated Ibu in industry relevant multicomponent blends and still feasible for DB-DC process.

However, for lower API loadings of 3 and 1 wt%, the dry coating formulations had to be more carefully selected to achieve the USP recommended stage 1 BU. The outcomes of these two papers (Huang et al., 2017; Kim et al., 2022b) suggest that the influence of factors to achieve acceptable BU at lower API loadings such as the agglomerate size distributions, mixing time and the relative sizes of the API and excipients, have not been examined before and need to be investigated.

Consequently, in this work, different mixing times, dry coating formulations, and relative sizes of the API and major excipients were investigated. Milled ibuprofen was selected as the model poorly water-soluble API. Two different excipient size classes were considered: a coarser class containing equal parts of Avicel PH102 and Pharmatose DCL11, a typical choice for conventional formulations, and a finer class containing equal parts of Avicel PH105 and Pharmatose 450, a dramatic contrast to general practice. Crospovidone and magnesium stearate (MgSt) were added as a disintegrant and lubricant, respectively. The mixing times varied from 5 to 60 min at a fixed mixing intensity (rotation speed) and filling degree. Four dry coating formulations were employed for milled Ibu: fixed surface area coverage (SAC) percent with either hydrophobic or hydrophilic silica and fixed wt% of either hydrophobic or hydrophilic silica. The interparticle cohesion reduction after dry coating (Castellanos, 2005; Chen et al., 2008; Dave et al., 2022b; Jallo et al., 2010; Kim et al., 2022a; Yang et al., 2005) was expressed by computing the dimensionless force ratio, granular Bond number ($Bo_g$) (Nase et al., 2001), for the individual components and their blends (Capece et al., 2015; Capece et al., 2014; Kunnath et al., 2021; Pasha et al., 2020). Blends containing either uncoated or dry coated Ibu at drug loadings of 1, 3, and 5 wt% with either coarse or fine excipients were prepared. The individual powder components and their multi-component blends were tested for flowability, bulk density, and agglomerate size. All prepared blends were assayed, and their tablets were analyzed for their API release rate. These comprehensive results, including the API and blend agglomeration, were analyzed to elucidate the significance of the relative excipient-API size differences, dry coating formulations, and mixing times on the blend uniformity as well as flowability, which is a major predictor of blend processability.

## 2. Materials and methods

### 2.1. Materials

Ibuprofen (Ibu), a poorly soluble drug, was selected (gift from BASF, USA) as the model API. The as-received Ibu ($d_{50}$ of 70 μm) was milled down to a finer size ($d_{50}$ ~ 15 μm) to observe the impact of particle cohesion variations with and without the dry coating. Microcrystalline cellulose (Avicel PH105 and Avicel PH102, gift from FMC Biopolymer, USA) and lactose (Pharmatose 450 and Pharmatose DCL 11, gift from DFE pharma, USA) were selected as a filler and binder, respectively. Crospovidone (Kollidon-CL, a gift from BASF, USA) was chosen as a disintegrant (Han et al., 2013a; Kunnath et al., 2018). Magnesium stearate (MgSt, Mallinckrodt Inc., USA) was selected as a lubricant. Aerosil A200 (nano-sized hydrophilic fumed silica) and Aerosil R972P (nano-sized hydrophobic fumed silica), gifts from Evonik Corporation (Piscataway, NJ, USA), were chosen as the dry coating materials (Kim et al., 2021). The properties of the excipients are presented in Table 1.

### 2.2. Methods

#### 2.2.1. Micronization: fluidized energy mill (FEM)

The as-received Ibu was micronized to a finer size ($d_{50}$ ~ 15 μm) using a fluidized energy mill (FEM, Pharmaceutical Micronizer Fluidized Energy Grinding Jet mill, Sturtevant Inc., Hanover, Massachusetts). FEM operating parameters, namely, *feeding rate, feeding pressure, and grinding pressure* that govern the final ground particle size, were set at 8 g/min, 30 psi, and 25 psi, respectively, based on previous work (Han et al., 2011; Han et al., 2013b). The details of the FEM operation may be found elsewhere (Han et al., 2011; Han et al., 2013b).

#### 2.2.2. Dry coating

Dry coating of the milled Ibu was performed using a material sparing high-intensity vibratory mixer (LabRAM, Resodyn, USA). Further details of the LABRAM operations may be found in the previous papers (Chen et al., 2018a; Chen et al., 2019). Based on the theoretical estimates of the surface areas of the host (API particle) and the guest (nano-fumed silica), the amount of silica required for a given weight of the API powders (~66 % by volume of the a standard 300 mL screw-top plastic container, equivalent to 30 to 40 g) were calculated, as shown in Eq. (1) (Yang et al., 2005).

$$\text{Weight percent of silica required}(\%) = \frac{SAC\ d_{guest}^3\ \rho_{guest}}{D_{host}^3\ \rho_{host}} \quad \frac{4\ D_{host}^2}{d_{guest}^2} \times 100 \tag{1}$$

Here, $D_{\text{host}}$ and $d_{\text{guest}}$ are the $d_{50}$ of milled API and the fumed nano-silica, respectively, while $\rho_{\text{host}}$ and $\rho_{\text{guest}}$ are the densities of the API and fumed nano-silica, respectively. The container filled with 30 to 40 g of the API powders along with the computed amount of nano-fumed silica was placed in LabRAM and mixed for 5 min at 75 times the gravitation force at 60 Hz. Two cases of dry coating formulations, the fixed 50 % surface area coverage (SAC) and the fixed 1 wt% were considered (Kim et al., 2022b). Ensuing dry coating formulation is presented in Table 2 (Kim et al., 2021; Kim et al., 2022a, 2022b).

**Table 1**
Properties of the blend components.

| Component | Mean particle size at 1.0 bar dispersion (μm) | Particle density (g/mL) |
|---|---|---|
| Milled Ibu (API) | 14.0 ± 0.2 | 1.14 ± 0.01 |
| Avicel PH105 | 18.9 ± 0.1 | 1.43 ± 0.01 |
| Avicel PH102 | 113 ± 0.1 | 1.60 ± 0.004 |
| Pharmatose 450 | 19.5 ± 1.7 | 1.48 ± 0.01 |
| Pharmatose DCL11 | 116 ± 0.1 | 1.60 ± 0.004 |
| Kollidon-CL | 38.0 ± 0.1 | 1.12 ± 0.01 |
| MgSt | 7.7 ± 0.2 | 1.01 ± 0.01 |
| R972P (hydrophobic nano fumed silica) | 0.018 | 2200 |
| A200 (hydrophilic nano fumed silica) | 0.012 | 2650 |

#### 2.2.3. Particle surface morphology analysis: Scanning Electron Microscopy

Image-based surface morphology analysis with Scanning Electron Microscopy (SEM) using EM JSM-7900F, JEOUL USA was performed for the milled Ibu with and without the dry coating, as well as the excipients for the purpose of qualitatively assessing the dry coating effectiveness (Kim et al., 2022a, 2022b). These surface SEM images are presented in the *Supplementary Materials*, Fig. S1 (a) through S1(k). Details of sample preparation for SEM imaging are maybe found elsewhere (Kim et al., 2021).

#### 2.2.4. Particle density

The particle densities of the components, including uncoated and dry coated Ibu10 and excipients, are measured and presented in Table 1. The particle densities of the coating materials were taken from the manufacturer's specifications. A Multipycnometer (P/N 02029-1, Quantachrome Instruments, USA) was used for the measurement of all other materials. Multiple measurements were taken to ensure repeatability under a helium environment. Assuming that the blends are ideal mixtures, Eq. (2) was used to calculate the particle densities of all prepared blends (Paul and Sun, 2017; Vreeman and Sun, 2021).

$$\rho_{\text{particle density of blend}} = \sum_{i=1}^{5} x_i \rho_i \tag{2}$$

In Eq. (1), each $x_i$ and $\rho_i$ denotes the mass fraction of component $i$ and particle density of component $i$, respectively.

#### 2.2.5. Blending: multi-component powder mixture

Mixing parameters such as the order of filling each constituent, fill level, mixing intensity, and mixing time were held constant (Alexander et al., 2004; Powderprocess, 2017), to prevent external impacts on the blend uniformity other than the API dry coating formulation and mixing time. The powder blend, without MgSt, was hand mixed prior to adding it to a 4-pint V-shaped container to minimize the impact from the component addition order to the container on the final mixedness (Axe, 1995; Shenoy et al., 2015). Hand-mixing involved adding the pre-weighted components to a 1-gallon Ziplock plastic bag, followed by gently shaking for five to ten seconds. The container fill level was kept at ~37 % by volume (equivalent to 280 g of powder blends) for all cases. While the mixing time varied from 5, 10, 15, 20, 30, 40, and 60 min, the rotation speed of the container was fixed at 25 rpm. Special care was taken when adding MgSt into the mixture to minimize its tendency to coat the other components (Bolhuis et al., 1981; Han et al., 2013a; Kunnath et al., 2018). Hence, MgSt was added to the V-blender container during the last 90 s of mixing. The resulting multi-component formulation details are presented in Table 3, where all four silica coating formulations are considered for 5 wt% blends, but only two best cases for either 3 or 1 wt% blends. That is because for lower drug concentrations, acceptable blend uniformity is more challenging to achieve

**Table 2**
Dry coating formulation for milled Ibu (Fixed % SAC equivalent to 50 % SAC for each silica case, fixed wt% corresponds to 100 % SAC of R972P and 177% SAC of A200).

| Case | Coating materials | wt% | API | wt% |
|---|---|---|---|---|
| Fixed % SAC | R972P | 1.16 | Milled Ibu | 98.84 |
| | A200 | 0.65 | | 99.35 |
| Fixed wt% | R972P | 2.31 | | 97.69 |
| | A200 | 2.31 | | 97.69 |

**Table 3**
Details of the blend formulations.

| | | | 5 wt% loading | | | | | 3 wt% loading | | | 1 wt% loading | | |
|---|---|---|---|---|---|---|---|---|---|---|---|---|---|
| | | | | Fixed wt% dry coating | | Fixed % SAC (50 % SAC) dry coating | | | Fixed wt % dry coating | Fixed % SAC (50 % SAC) dry coating | | Fixed wt % dry coating | Fixed % SAC (50 % SAC) dry coating |
| | | Placebo | Uncoated | R972P | A200 | R972P | A200 | Uncoated | A200 | R972P | Uncoated | A200 | R972P |
| Coarse excipient blends | API | 0 | 5 | 5 | 5 | 5 | 5 | 3 | 3 | 3 | 1 | 1 | 1 |
| | R972P | 0 | 0 | 0.116 | 0.000 | 0.058 | 0.000 | 0 | 0.000 | 0.035 | 0 | 0.000 | 0.012 |
| | A200 | 0 | 0 | 0.000 | 0.116 | 0.000 | 0.033 | 0 | 0.069 | 0.000 | 0 | 0.023 | 0.000 |
| | Avicel PH102 | 47 | 44.5 | 44.4 | 44.4 | 44.5 | 44.5 | 45.5 | 45.5 | 45.5 | 46.5 | 46.5 | 46.5 |
| | Pharmatose DCL11 | 47 | 44.5 | 44.4 | 44.4 | 44.5 | 44.5 | 45.5 | 45.5 | 45.5 | 46.5 | 46.5 | 46.5 |
| | Kollidon-CL | 5 | 5 | 5 | 5 | 5 | 5 | 5 | 5 | 5 | 5 | 5 | 5 |
| | MgSt | 1 | 1 | 1 | 1 | 1 | 1 | 1 | 1 | 1 | 1 | 1 | 1 |
| | Total wt% | 100 | 100 | 100 | 100 | 100 | 100 | 100 | 100 | 100 | 100 | 100 | 100 |
| Fine excipient blends | API | 0 | 5 | 5 | 5 | 5 | 5 | 3 | 3 | 3 | 1 | 1 | 1 |
| | R972P | 0 | 0 | 0.116 | 0.000 | 0.058 | 0.000 | 0 | 0.000 | 0.035 | 0 | 0.000 | 0.012 |
| | A200 | 0 | 0 | 0.000 | 0.116 | 0.000 | 0.033 | 0 | 0.069 | 0.000 | 0 | 0.023 | 0.000 |
| | Avicel PH105 | 47 | 44.5 | 44.4 | 44.4 | 44.5 | 44.5 | 45.5 | 45.5 | 45.5 | 46.5 | 46.5 | 46.5 |
| | Pharmatose 450 | 47 | 44.5 | 44.4 | 44.4 | 44.5 | 44.5 | 45.5 | 45.5 | 45.5 | 46.5 | 46.5 | 46.5 |
| | Kollidon-CL | 5 | 5 | 5 | 5 | 5 | 5 | 5 | 5 | 5 | 5 | 5 | 5 |
| | MgSt | 1 | 1 | 1 | 1 | 1 | 1 | 1 | 1 | 1 | 1 | 1 | 1 |
| | Total wt% | 100 | 100 | 100 | 100 | 100 | 100 | 100 | 100 | 100 | 100 | 100 | 100 |

(Huang et al., 2017; Kim et al., 2022b).

### 2.2.6. Surface energy analysis

Automated inverse gas chromatography (SEA-IGC, Surface Energy Measurement System Ltd., UK) was used to measure the surface energy of the uncoated, dry coated Ibu and excipients before blending. The infinite dilution method was employed where the surface energy was evaluated via Lifshitz-van der Waals (LW) method (Lavielle and Martin, 1987). The details of sample preparation and analysis methods, including nonpolar and polar probes lists may be found elsewhere (Han et al., 2013b; Kim et al., 2021, 2022a).

### 2.2.7. Primary and agglomerate particle sizing

Two different particle sizing methods were adopted to assess their primary sizes and naturally agglomerated state (Kim et al., 2021, 2022b). Primary particle sizes were measured using a compressed dry air dispersion and a laser diffraction particle sizer (Rodos/Helos, Sympatec, USA). The dispersion pressure was determined to be 1.0 bar based on pressure titration results by testing the measurement consistency as the compressed air pressure varied from 0.1 to 2 bar. As reported in the previous studies, the change in the agglomerate size of the dry coated cohesive API was not discernible even at the lowest dispersion pressure using Rodos/Helos system (Huang et al., 2017; Kim et al., 2021), likely because even the lowest dispersion pressure led to nearly complete deagglomeration for both uncoated and dry coated powders. Consequently, Helos/Rodos laser diffraction particle size analyzer was only used to measure primary particle sizes (Huang et al., 2017; Kim et al., 2021; Kunnath et al., 2018).

More reliable quantification of the agglomerate size was done by using Sympatec Gradis/QicPic, a dynamic imaging particle sizer (Sympatec Inc., NJ) (Allenspach et al., 2020; Stavrou et al., 2020; Zakhvatayeva et al., 2018; Zuo et al., 2019). Gradis relies on gravity to disperse the powders as they fall through a 50 cm long shaft passing the camera window, allowing the dynamic imaging analyzer, QicPic, to gather 2-D images of powder in real-time and converting the image data to measurement and shape data (Allenspach et al., 2020; Stavrou et al., 2020; Zakhvatayeva et al., 2018; Zuo et al., 2019). For each test, the sample size was 2 to 4 g of powders, fed by combinations of the gravity and the vibration of the attached vibrational V-shaped feeding tray (VIBRI). A maximum of 30 % of the vibrational capacity of the VIBRI was used to avoid excessive disturbance of the natural agglomerates. The vibration setting was kept consistent throughout the measurements. The test typically lasted 10 *sec* allowing the approximate feeding rate to be 0.2–0.4 g/*sec*. Thus, the testing ensured the collection of a statistically significant number of sample images, which could include as many as $\sim 10^7$ particle images, thus well representing the entire population PSD of the sample (Allenspach et al., 2020; Borchert and Sundmacher, 2011; Neugebauer et al., 2018; Stavrou et al., 2020; Yu and Hancock, 2008).

### 2.2.8. Bulk powder properties assessment: flowability and bulk density

Bulk powder density, bulk powder cohesion at zero normal force, and powder flowability via shear testing were measured with a powder tester (FT4, Freeman Technology, UK). For the bulk powder density measurement, an acrylic 25 mL cylinder was used, while bulk cohesion and flowability were measured in an acrylic 10 mL cylinder. Both containers had an internal diameter of 25 mm. The pre-shear normal stress of 3 kPa was held consistently throughout all relevant assessments. The powder flowability was expressed as Flow Function Coefficient, FFC, the ratio between the major principal stress and unconfined yield strength (Freeman, 2007), giving rise to the flow regimes as follows: no flow ($0 < FFC < 1$), very cohesive ($1 < FFC < 2$), cohesive ($2 < FFC < 4$), easy-flow ($4 < FFC < 10$), and free-flow ($10 < FFC$) (Schulze et al., 2008). Details of the FT4 testing maybe found elsewhere (Huang et al., 2017; Kim et al., 2021).

### 2.2.9. Blend uniformity: API concentration assay

The blends mixedness was evaluated based on API concentration assay. The blend sampling was done using a spinning riffler equipped with 16 sampling tubes (ST-230, Gilson Company, Inc, USA) (Garcia et al., 2015; Huang et al., 2017; Kim et al., 2022b). An entire bag, filled with the blend subject to testing, was emptied into the spinning riffler and the sampling was done multiple times to ensure random testing per formulation and mixing time. For each run, one of the 16 collection tubes was selected randomly and poured selected tube onto the spinning riffler again to further divide and sample. The divide and sample processes were repeated until the powder sample was reduced down to <2 g of powder per 16 test tubes. A tube was randomly selected and 400 mg of powder was taken, dissolved in 100 mL of pH 7.2 phosphate buffer, and

magnetically stirred for 24 h. After 24 h, 5 mL of liquid samples were taken from the prepared 100 mL with a syringe filter, which then was diluted by adding 20 mL of pH 7.2 phosphate buffer. The concentration of the extracted API during the assay test was measured through the absorbance at 221 nm wavelength, then converted to concentration (mg/L) based on a pre-determined calibration curve. A UV–visible spectrophotometer (Thermo Scientific, USA) was employed for the absorbance measurement. For each sample, the absorbance was measured in triplicate to check for repeatability.

For assessing the mixedness of the samples, <USP 905 > general chapter's guideline (USP-NF, 2011) was used and the outcomes were reported via the API concentration's relative standard deviation (*RSD*, see Eq. (3)) as done in several other references (Bergum et al., 2014; Bridgwater, 2012; Huang et al., 2017; Senderak, 2009).

$$RSD(\%) = \frac{\text{Standard Deviation of the tested samples' API content}}{\text{Average of the API content measured from the samples}} \times 100 \tag{3}$$

The blend uniformity was discerned based on % *RSD* which was deemed to be more suitable for comparative purposes during research and development stage. This is in line with previous reports which also only reported % *RSD*, since its higher values also indicate failure to meet the acceptance value requirements of the blends (Muzzio et al., 1997; Sierra-Vega et al., 2019; Sun et al., 2017; Vanarase et al., 2013).

For each powder blend, 10 samples were tested initially to determine if the dosage per sample is within 90–110 % of the target dosage (stage 1, as per <USP 905>). The API concentration *RSD* was calculated using Eq. (3) to check if % *RSD* was <6 %. If both the criteria from stage 1 were satisfied, the blend was considered to pass the minimum requirement to be believed as uniform. If not, 20 additional samples were analyzed in a similar manner (Huang et al., 2017; Johnson, 1972; Kim et al., 2022b).

#### 2.2.10. Tablet preparation

Carver platen press (Carver, Inc., USA) with a 12.7 mm inner diameter stainless die and a flat-faced round punch was used to prepare 400 mg tablets under 78 MPa and 155 MPa (equivalent to 1.0 and 2.0 metric tons) compaction pressure for fine and coarse blends respectively to match their tensile strength at about 2.0 MPa (Kunnath et al., 2018; Sun, 2008). The die set was cleaned thoroughly with alcohol wipes and air-dried before and after. The tablets were tested for their tensile strength and Ibu release rates. Tablet weight uniformity was neither relevant nor assessed since the powders were from the same spinning riffler sampling method to make the tablets and perform the API concentration assays.

#### 2.2.11. Tablet tensile strength and moisture content analysis

The tablet tensile strength and moisture content were assessed since they have an impact on the tablet disintegration rate and drug release rate (Gordon et al., 1993; Sun, 2008; Zaborenko et al., 2019). Tablet breaking force (Fell and Newton, 1970) was measured using a diametrical compression test in a texture analyzer (Texture Technologies Corp., USA), and converted to the tablet tensile strength via Eq. (4).

$$\sigma_T = \frac{2 \times F}{\pi D_T \delta_T} \tag{4}$$

In the above equation, $\sigma_T$, $F$, $D_T$, and $\delta_T$ represent tensile strength of tablet, tablet breaking force measured, diameter of the tablet, and thickness of the tablet, respectively. For each formulation, an average of a minimum of 10 tablets was used.

A thermogravimetric analyzer (TGA, TGA/DCS1/SF START$^e$ system, Mettler Toledo Inc., USA) was used to measure the tablet moisture content. About 30 to 50 mg of samples were taken by breaking 400 mg tablet right before the measurement and placed in a ceramic crucible. The sample was heated in the nitrogen environment from 25 °C to 200 °C at the temperature rising rate of 10 °C per min, during which the change in its mass was recorded automatically. The measurements were done in triplicate to check for repeatability.

#### 2.2.12. API release rate analysis

As per USP ⟨711⟩ guideline, the API release rates from the tablets were tested via the USP II paddle method (USP II, SOTAX, Switzerland). The system temperature and the paddle rotating speed were fixed at 37 °C ± 0.2 °C and 50 rpm, respectively, during the test. The ibuprofen solubility in PBS pH 7.2 buffer was measured to be 2 mg/mL at the ambient condition. Hence, 500 mL pH 7.2 phosphate buffer was used as the dissolution medium to ensure sink condition throughout the testing. This allowed sufficient API concentration detection via UV–vis analysis without further dilution (UV–vis spectrometer, Thermo Scientific, USA). At the pre-determined time intervals, 3 mL of samples were drawn while replenishing the buffer amount by adding 3 mL of make-up solvent. The absorbance of the sample was measured in duplicate at the wavelength of 221 nm after filtering the collected 3 mL with a 0.45 μm syringe filter. At least three tablets per formulation were tested to check for repeatability in the Ibu release rate trend.

## 3. Results and discussion

Individual powder properties such as primary and agglomerated particle sizes, flowability (FFC), bulk density, and their granular Bond number were analyzed prior to the blend properties assessments. Before discussing details of the experimental results and discussion, a schematic process flow diagram to illustrate the comparison between the current approach and the novel paradigm-shifting approach from powder mixing to tableting and the resulting impact on the bulk powder blend properties is shown in Fig. 1 (a) and 1(b).

### 3.1. Properties of individual powders

The normalized agglomerate size was calculated by taking the ratio of the mean agglomerated particle size measurement from Gradis/QicPic and the mean primary particle size measurement from Rodos/Helos. The normalized agglomerate size or the agglomerate ratio (AR) for the individual powders and their associated primary particle sizes are shown in Fig. 2. The greater agglomeration tendency with smaller powders is evident in Fig. 2, where the weak long-range force, $F_{VdW}$, plays the dominant role in the increased particle cohesiveness (Castellanos, 2005; Nase et al., 2001). Interestingly, the dry coated APIs show a significant reduction in the AR, close to the coarse excipients, inferring that dry coating had notably reduced the effect from $F_{VdW}$, thus reducing interparticle cohesion force. Next, the bulk properties of the individual powders, measured to analyze the effect of the size and the dry coating, are presented.

#### 3.1.1. FFC and BD of individual powders

The flowability (FFC) and bulk density (BD) of individual powders are presented in Fig. 3. The green dotted reference lines for FFC and BD have been the values recommended as the bars for direct compressibility and have also been confirmed by our industry collaborators (Sun, 2010). As expected, coarse excipients, Avicel PH102 and Pharmatose DCLII, exhibited free-flowing behavior, whereas the fine excipients, Avicel PH105 and Pharmatose 450, as well as the uncoated fine milled API exhibited poor flow behavior, either a very cohesive or cohesive flow range. In contrast, dry coated fine milled API achieved dramatically enhanced flowability, as good as or better than the free-flowing coarse excipients (see Fig. 3). The observed improvements agree with the remarkable agglomerate reduction of the dry coated APIs shown in Fig. 2. Specifically, the FFC was at or above the value 10, indicating a free-flowing regime for either formulation consisting of R972P coating, whereas the FFC was just under 10 for A200 formulations, yet comparable to the FFC of Avicel PH102. The significant flow enhancements achieved with various dry coating formulations for fine milled Ibu could

(a)

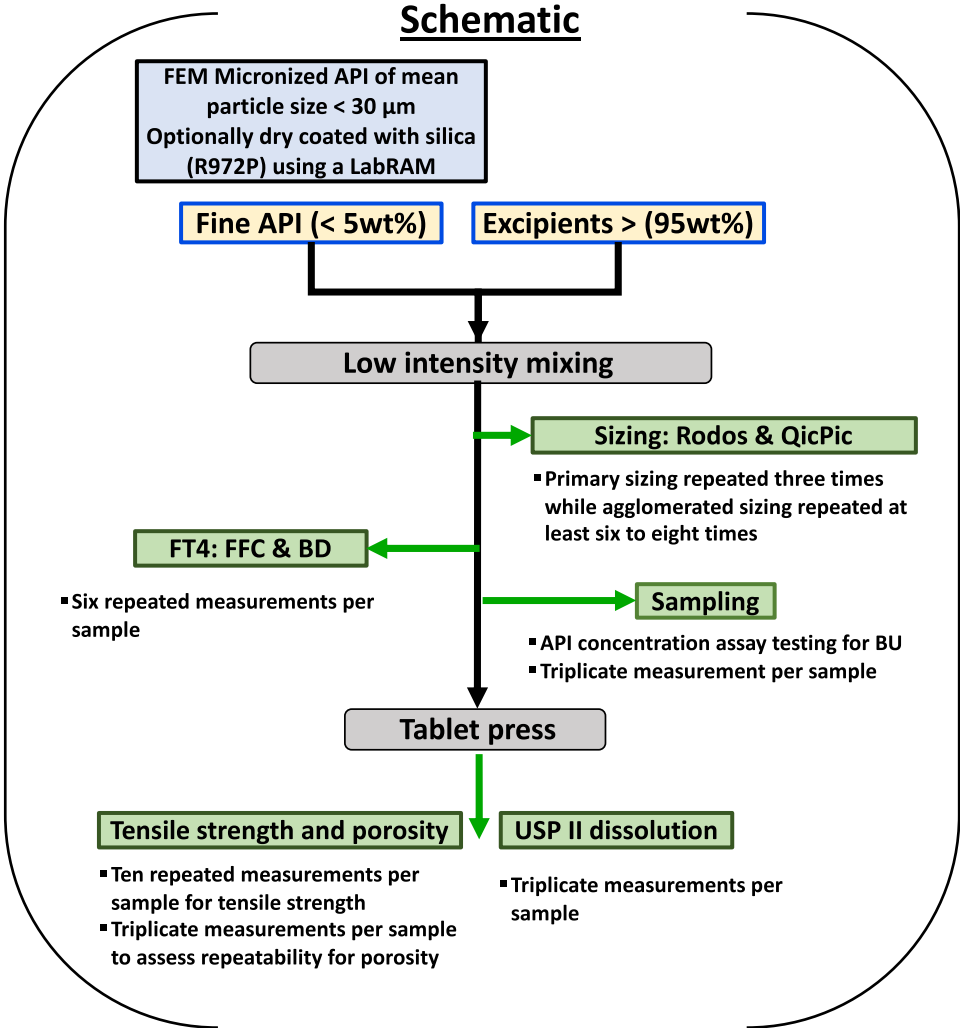


(b)

| Conventional Approach | New Paradigm Shifting Approach |
|---|---|
| Well flowing larger sized excipients (≥ 95 wt%) | Finer excipients (≥ 95 wt%) |
| Fine API (≤5 wt%) | Fine dry coated API (≤5 wt%) |
| **Results**<br>○ Blend FFC ≤ Placebo FFC<br>○ Agglomerated API hence BU and tablet CU fails, poor dissolution from tablets<br>○ Need for wet granulation | **Results** (despite silica ≤ 0.02 wt % in the blend/tablet)<br>○ Blend FFC ≫ Placebo FFC due to synergy<br>○ Non-agglomerated API hence BU and tablet CU pass, excellent dissolution from tablets<br>○ Direct blend direct compression (DB-DC) ready |

**Fig. 1.** (a) Schematic process flow. The grey and green boxes represent process and testing, respectively. (b) Conventional versus novel paradigm shifting approach. (For interpretation of the references to colour in this figure legend, the reader is referred to the web version of this article.)

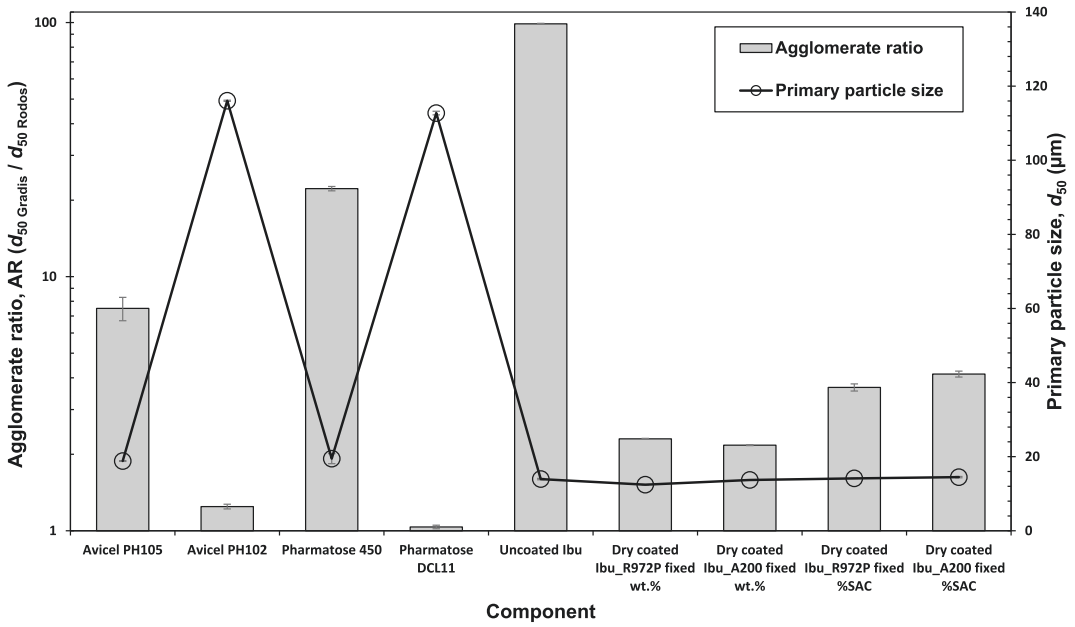


**Fig. 2.** Agglomerate ratio (AR) and primary particle sizes of the individual powders including the major excipients, uncoated and dry coated APIs.

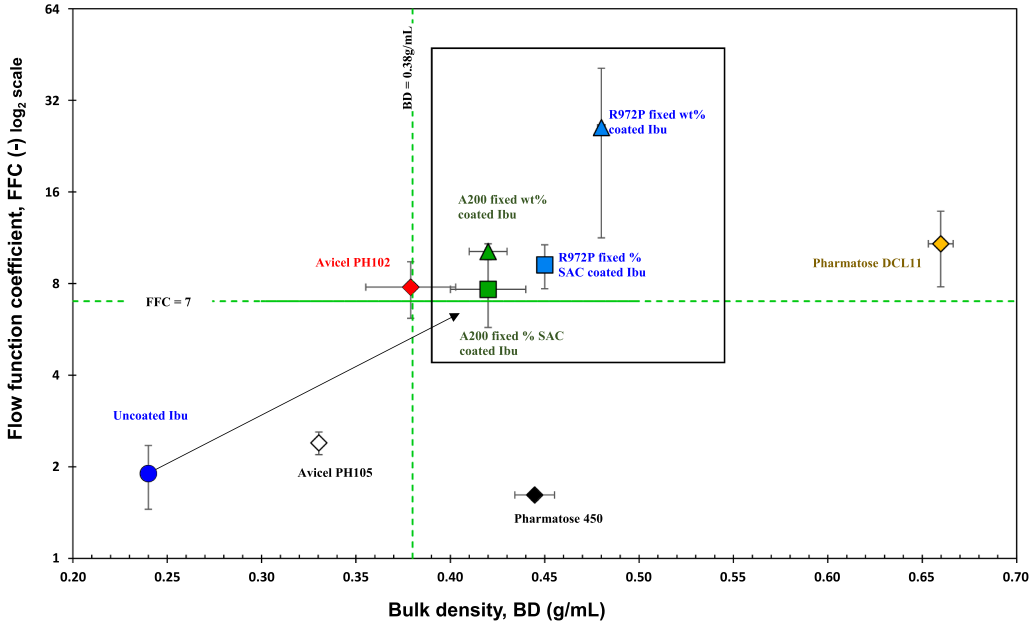


**Fig. 3.** The phase map of bulk powder flowability (FFC) and bulk density (BD) for individual powders. Green dotted lines help denote the top-right quadrant that is favorable for direction compaction (FFC > 7, BD > 0.38 g/mL). Each measurement was repeated six times to assure reproducibility. (For interpretation of the references to colour in this figure legend, the reader is referred to the web version of this article.)

be explained based on the drastic impact on the relative cohesion, characterized by over an order of magnitude reduction in the granular Bond number discussed next.

### 3.1.2. $Bo_g$ of individual components and its relation to FFC and AR

The granular Bond number, $Bo_g$, a dimensionless parameter to characterize reduced particle contact force, may be calculated as follows.

$$Bo_g = \frac{F_{vdW}}{\frac{\pi}{6}D^3\rho_p\ g} \tag{5}$$

where $\rho_p$ is the particle density and $D$ is the primary particle diameter.

The interparticle cohesive force ($F_{vdW}$) may be estimated using the multi-asperity Chen et al. model (Chen et al., 2008), as per Eq. (6). For uncoated particles, Eq. (6) accounts for the contact force between two spherical particles with evenly distributed naturally present surface asperities.

$$F_{vdW} = \frac{A}{12z_0^2}\left[\frac{d_{asp}D}{d_{asp}+D} + \frac{D}{\left(1+d_{asp}/2z_0\right)^2}\right] \tag{6}$$

Here, $D$ and $d_{asp}$ are the primary particle size and natural asperity, respectively, $z_0$ is the atomic separation distance (0.4 nm) between two surfaces and $A$ is the Hamaker constant which can be calculated based on the experimentally measured dispersive surface energy ($\gamma_d$) and

minimum separation distance ($D_0$, assumed to be 0.165 nm) as shown in Eq. (7).

$$A = 24\pi(\gamma_d^2)D_0 \tag{7}$$

The natural asperity size, $d_{asp}$, has been suggested to be 200 nm (Massimilla and Donsì, 1976) or it could be estimated as a function of the host particle size (Yu et al., 2003), Eq. (8), for uncoated milled API or as-received excipients.

$$d_{asp} = a(D)^b \tag{8}$$

In the above equation, α and β are fitting parameters, shown to work well for uncoated powders using β = 0.6, and α = 0.0004 $m^{0.4}$ (Capece et al., 2014; Yu et al., 2003).

For dry coated powders, the natural asperity size could be replaced by the guest particle size, hence the Chen multi-asperity model (Chen et al., 2008) may be expressed as Eq. (9). It is assumed that the amount of nano-silica particles is sufficient to assure guest–guest contacts, which is likely to be the case as per the silica amounts used and qualitative inspection of the SEM images in Fig. S1 (b) through S1(e) in the *Supplementary Materials*.

$$F_{vdW} = \frac{A d_{guest}}{8 z_0^2} + \frac{A\ D_{host}}{24\left(2\ d_{guest} + z_0\right)^2} \tag{9}$$

The $Bo_g$ values for individual components along with their FFC and AR values are presented in Fig. 3. As expected, there is a negative correlation between $Bo_g$ and FFC such that a higher FFC corresponds to a lower $Bo_g$ and vice versa (Capece et al., 2015; Kim et al., 2022a; Kunnath et al., 2021). Likewise, a power-law relationship between $Bo_g$ and AR is evident, noting that an increase in the particle cohesiveness ($Bo_g$) increases the likelihood of forming large agglomerates and causes poor flow (Castellanos, 2005; Kim et al., 2022a; Yang et al., 2005). Interestingly, $Bo_g$ of the milled API was reduced by one to two magnitudes after dry coating, though still greater than the $Bo_g$ of Avicel PH102 and Pharmatose DCL11. Remarkably, the AR values of dry coated APIs were comparable to those of two coarse, free-flowing excipients, suggesting a marginal difference in their flow behavior. Moreover, this behavior is a significant enhancement confirmed by equal or higher FFC values for the APIs as they increased from the low FFC of ~1.5 to as high as ~26 after dry coating (see the *Supplementary Materials* Fig. S2). It is important to note that the close correspondence between low AR and high FFC for dry coated APIs serves as direct evidence that the benefit of the dry coating could not be fully captured by the $Bo_g$. The combined effect of the imparted nano-scale roughness due to dry coating and the low surface energy of the coating material has been demonstrated before and seen from Eqs (1) and (9), greatly reduces the cohesion between coated particles, leading to enhanced flowability see Table S3 *Supplementary Materials*, (Chen et al., 2008; Han et al., 2013b; Kim et al., 2022a; Yang et al., 2005).

In summary, approximate power-law relation between the FFC and AR was observed for individual powder components, such as the Ibu with and without dry coating and main excipients; see Fig. 4 and Fig. S2 in the *Supplementary Materials*, in agreement with previous work (Kim et al., 2022a).

### 3.2. Blend uniformity as a function of the mixing time

At low drug loading, the impact of the API flowability on blend's mixedness as a function of the mixing time is assessed next for all three drug loading cases with and without dry coating at varying levels and types of silica. The first set of results are for blends consisting of uncoated API, followed by those with dry coated API.

#### 3.2.1. Blends with uncoated API

The % *RSD* of API concentration, representing the blend mixedness, for 5 wt% loaded blends are plotted in Fig. 5(a) for coarse excipient blends and Fig. 5(b) for fine excipient blends (see *Supplementary Materials*, Table S1 for detailed %*RSD* results). The blend uniformity of uncoated API blends failed to reach the acceptable level, which could have been expected. However, the blend uniformity was relatively better for the coarse excipient blend at all mixing times. The trend was the same for 3 and 1 wt% API loaded blends, see Fig. 5(c) through 5(f). Better blend uniformity attained by coarse excipients appears to contradict well documented segregation tendency of disparate size powders having size ratio of two or greater (Gray and Thornton, 2005; Jullien and Meakin, 1990; Ottino and Khakhar, 2000; Tang and Puri, 2004). However, the well-known size-driven segregation behavior is only applicable to non-cohesive, freely flowing powders. Therefore, it is not applicable

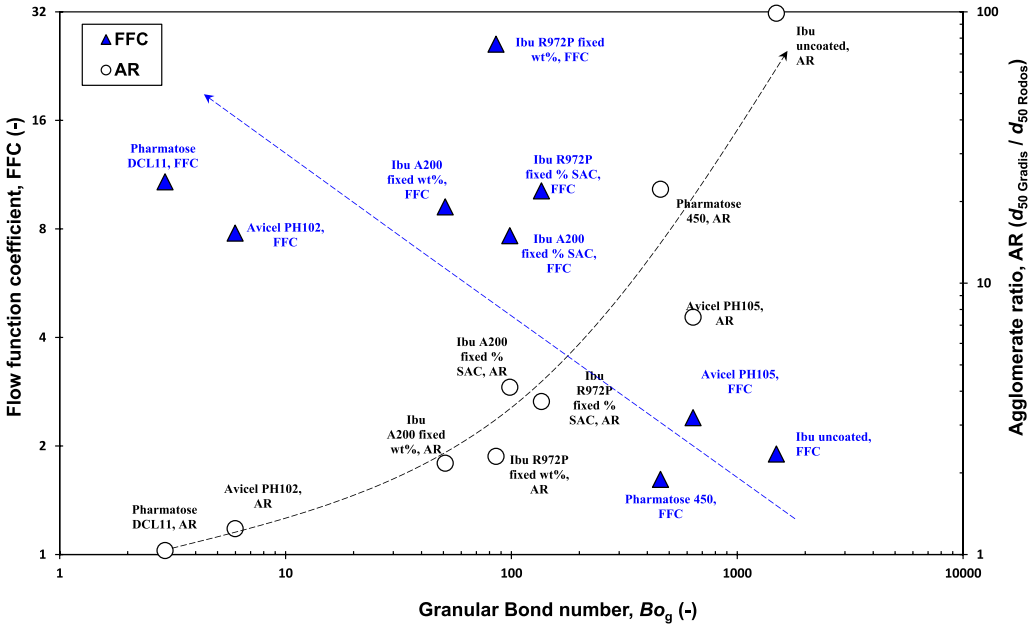


**Fig. 4.** The granular Bond number ($Bo_g$, $\log_{10}$ scale), flowability (FFC, $\log_2$ scale) and agglomerate ratio (AR, $\log_5$ scale) of the major excipients and API without and with dry coating. Two illustrative trend lines intended to help visualize the relationship between $Bo_g$-FFC and $Bo_g$-AR.

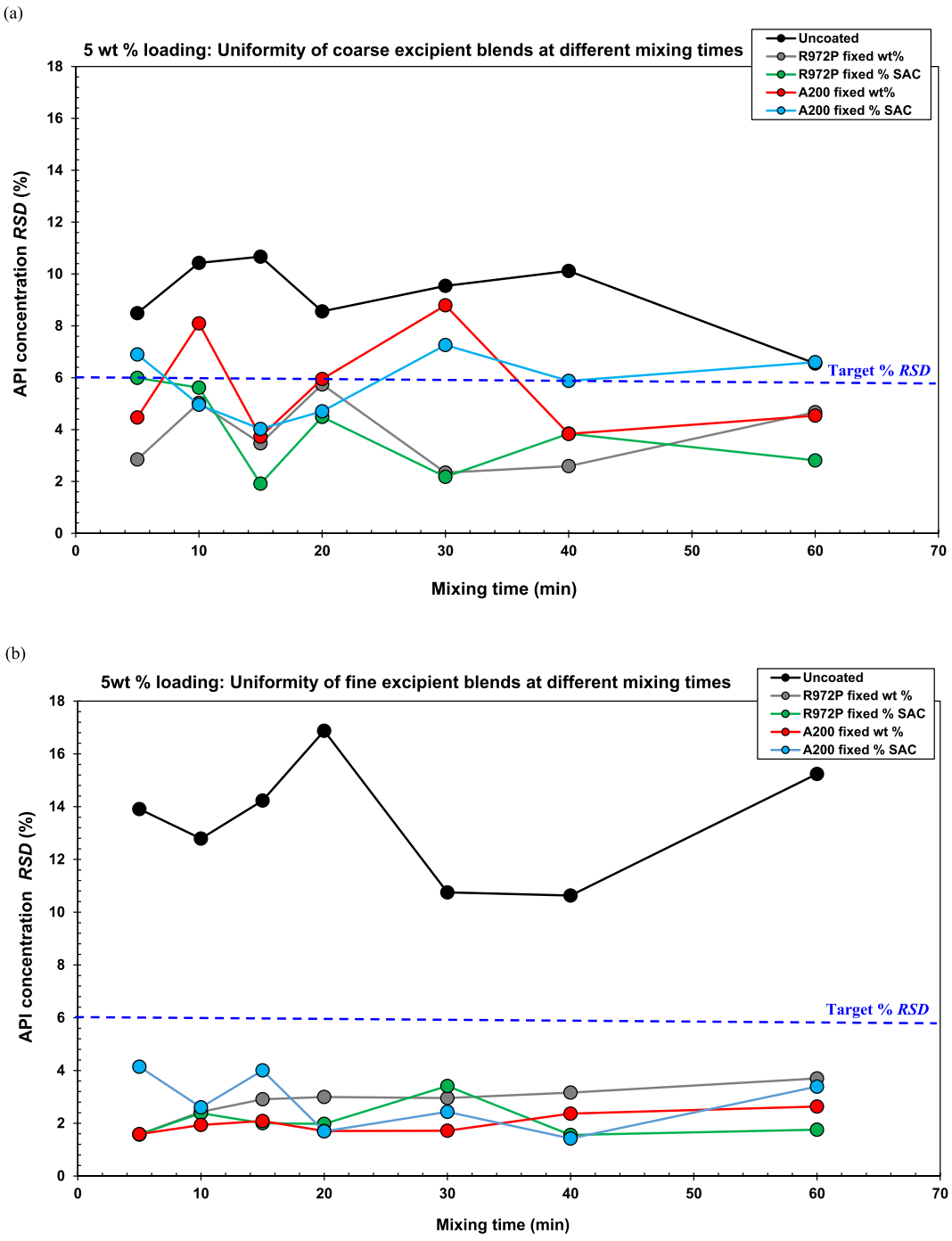


**Fig. 5.** Relative mixedness of the blends with either uncoated or dry coated API at different mixing times: (a) 5 wt% coarse excipient blends, (b) 5 wt% fine excipient blends, (c) 3 wt% coarse excipient blends, (d) 3 wt% fine excipient blends, (e) 1 wt% coarse excipient blends, and (f) 1 wt% fine excipient blends. Samples with %*RSD* below 6% were considered to pass the minimum homogeneity test.

to cohesive, uncoated fine API blends. In case of cohesive API blends with fine excipient powders, it is clearly not applicable, and high % *RSD* for fine excipient and fine API blends could have resulted from large API agglomerate formation, see Fig. 2 and Table S2, *supplementary material*, as well as inability of the fine excipients to break down API agglomerates during blending. However, the blends comprised of cohesive, uncoated fine API and coarse, nearly non-cohesive excipient powders of Fig. 5(a), 5(c), and 5(e), it is likely that the fine API powders could have behaved like larger agglomerated powders having roughly similar size as that of coarse excipients, leading to lower segregation tendency and relatively better mixing driven by coarser excipients. Nonetheless, regardless of the size of the excipients, fine cohesive API blends could not achieve the required mixedness, likely due to formation of large agglomerates induced by high cohesion.

### 3.2.2. *Blends with the dry coated API*

Dramatic improvement in 5 wt% API blend uniformity of both coarse and fine excipient blends was observed for the dry coated fine API powder, which is in stark contrast with the uncoated API blends. Remarkably, all fine excipient blends achieved significant improvement,

(c)

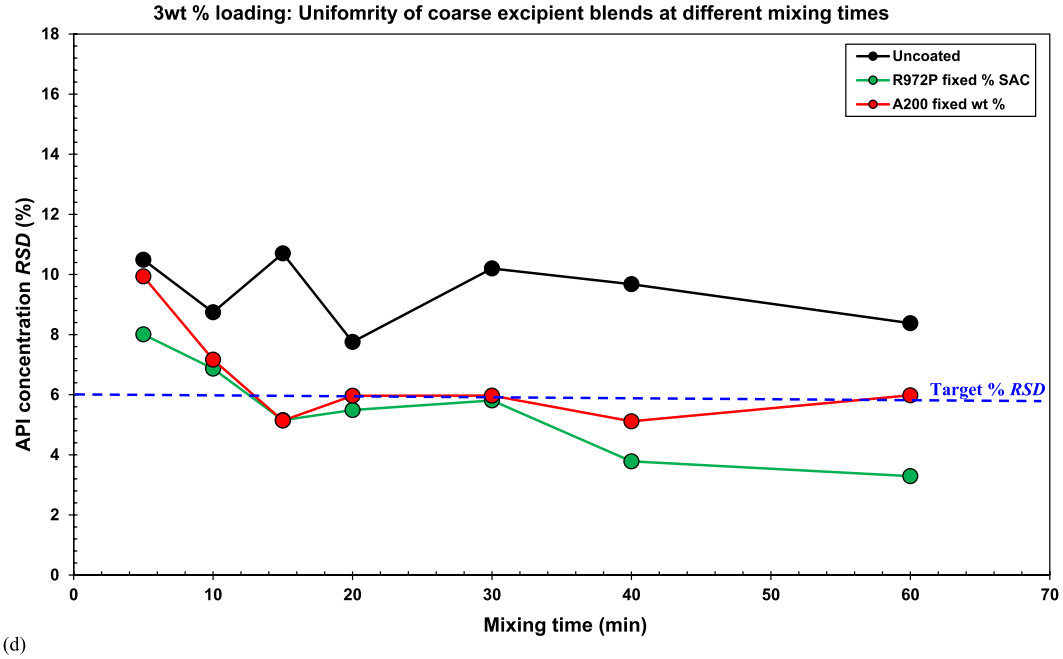


(d)

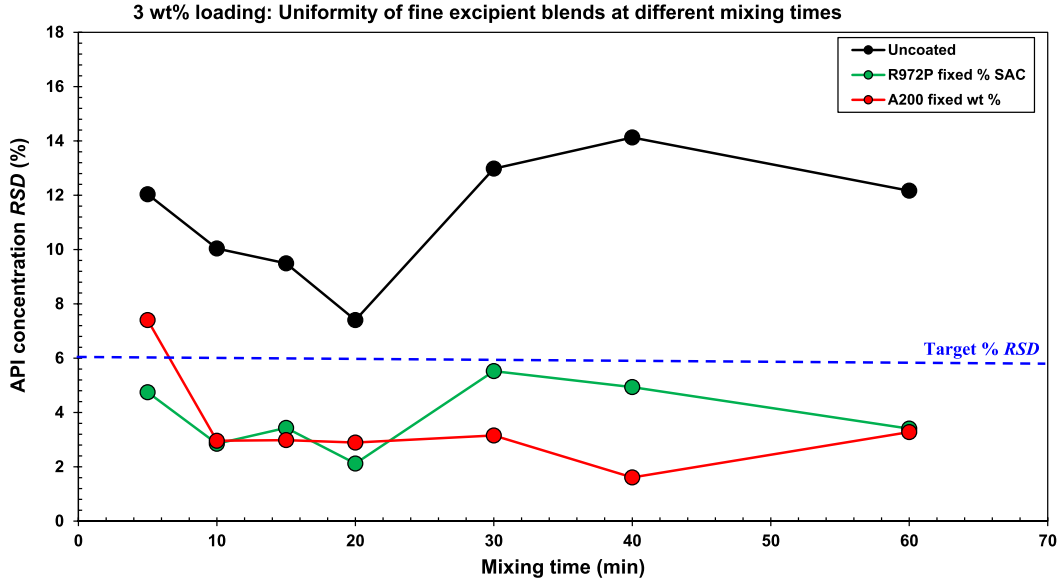


**Fig. 5.** (*continued*).

independent of the dry coating formulation, meeting the target % *RSD* at mixing times as low as 5 min. In contrast, the coarse excipient blends at 5 wt% API required longer mixing times than those of fine excipient blends to meet the target % *RSD*, see Fig. 5(a). The best two out of the four 5 wt% API blend dry coating formulations were selected for subsequent investigation for the 3 and 1 wt% API blends. Also, these cases experienced significant blend uniformity improvement, except at the lowest API loading whereA200 coated blends required longer mixing times to reach desired *RSD* values, generally in line with previously reported trends (Huang et al., 2017; Kim et al., 2022b). Such positive outcomes could be attributed to the significant agglomerate size reduction for the dry coated API, see Fig. 2. The 3 or 1 wt% dry coated API fine excipient blends follow a similar trend as the 5 wt% fine excipient blend, requiring shorter mixing times than the coarse excipient blends to meet the target % *RSD*.

In summary, the results presented in Fig. 5(a) through 5(f), in conjunction with the API agglomeration results in Fig. 2, demonstrate the importance of the state of API agglomeration to the blend uniformity. Remarkably, reducing API agglomeration could help improve the blend homogeneity even at the lowest 1 wt% API loading.

### 3.3. Blend properties: flowability and agglomerates

Next, the bulk powder properties, flowability (FFC) and agglomeration (AR) of the of 5 wt% and 1 wt% blends, representing the most challenging and the least challenging fine excipient blends formulations from a bulk flowability perspective were examined. The 3 wt% blends were purposely omitted from the analysis to fully dedicate the current manuscript to exploring these two extreme cases and to avoid redundancy in analysis. For the sake of completeness, the flowability of the coarse excipient 5 and 1 wt% API loaded blends are presented in the *Supplementary Materials*, Fig. S3(a) and S3(b). This section concludes

(e)

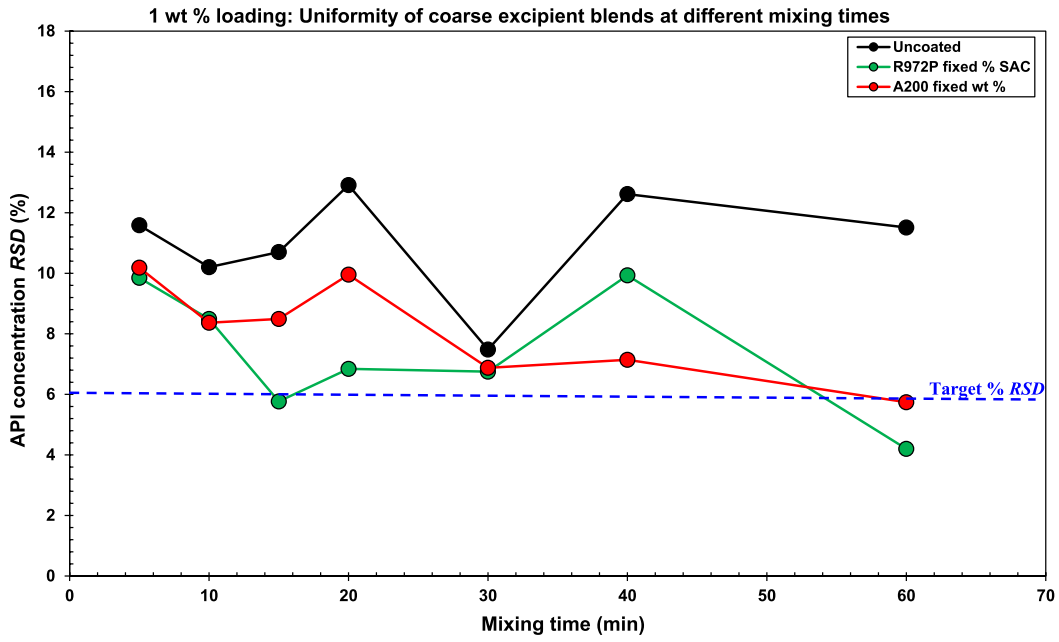


(f)

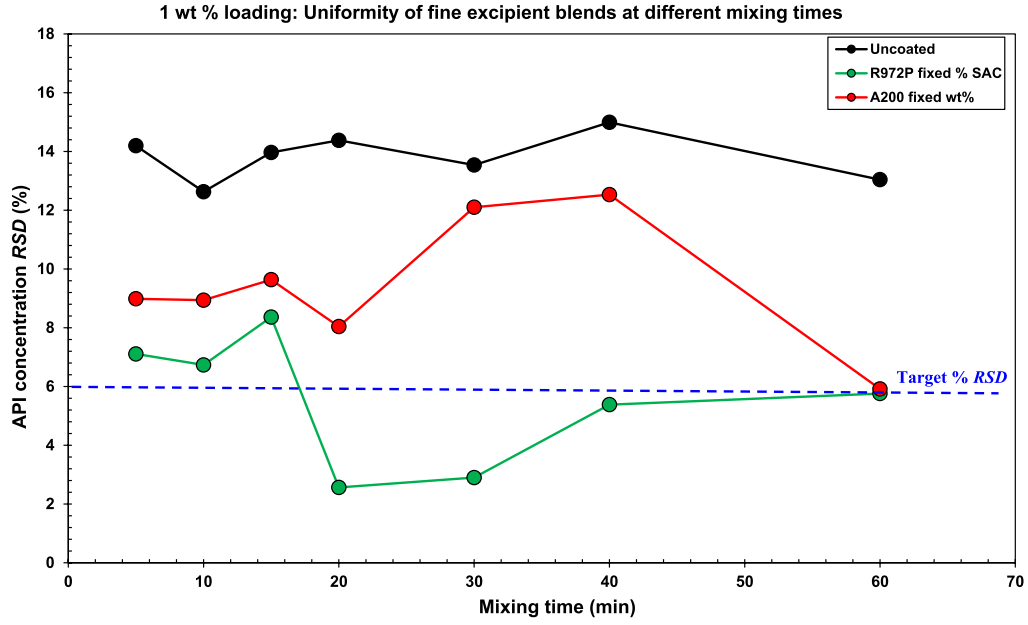


**Fig. 5.** (*continued*).

with plots that depict the relationship between the agglomerate ratio (AR) and the flowability (FFC) of the blends at various mixing times.

*3.3.1. Flowability at different mixing times: 5 wt% and 1 wt% API loadings*

Fig. 6(a) and 6(b) present bulk flowability of fine excipient blends at 5 and 1 wt% API loading, respectively, at differing mixing times. While good flow behavior at all mixing times of the coarse excipient blends was expected because of very low API loadings (see the *Supplementary materials* Fig. S3(a) and S3(b)), it was surprising to find significant bulk flowability improvements for fine excipient blends with dry coated Ibu, especially for 1 wt% API loading case (see Fig. 6(a) and 6(b)). It is noted that the FFC of the placebo blend (prepared by mixing for 30 min) was 3.5 and as expected, the FFC of the uncoated Ibu blends was similar, all corresponding to the cohesive flow category. In contrast, the FFC of the fine excipient blend of both dry coated Ibu formulations reached easy flow category after about 30 min of mixing time. Most interestingly, the 1 wt% dry coated Ibu blends even reached the level of greatly enhanced flowability since FFC values of 7.15 and 7.94, for R972P fixed SAC and A200 fixed wt%, respectively were attained at 30 min mixing times; note that the blend having FFC of about 7 and higher is high-speed direct compaction capable (Chen et al., 2019; Dave and Chen 2018; Huang et al., 2015a; Kunnath et al., 2018). These surprising and favorable flowability enhancements of fine excipient blends, in particular for 1 wt % blend, suggest existence of synergy due to some of the silica transferring from the API surfaces to excipients surfaces during mixing, in line with what has been mentioned in previous papers (Chen et al., 2019; Dave et al., 2022a; Kim et al., 2022b). It is remarkable that the total silica wt % in these blends was as low as 0.012 wt%, yet the impact on flowability was profound. The flow improvement of these blends from cohesive to the easy-flowing range may promote subsequent

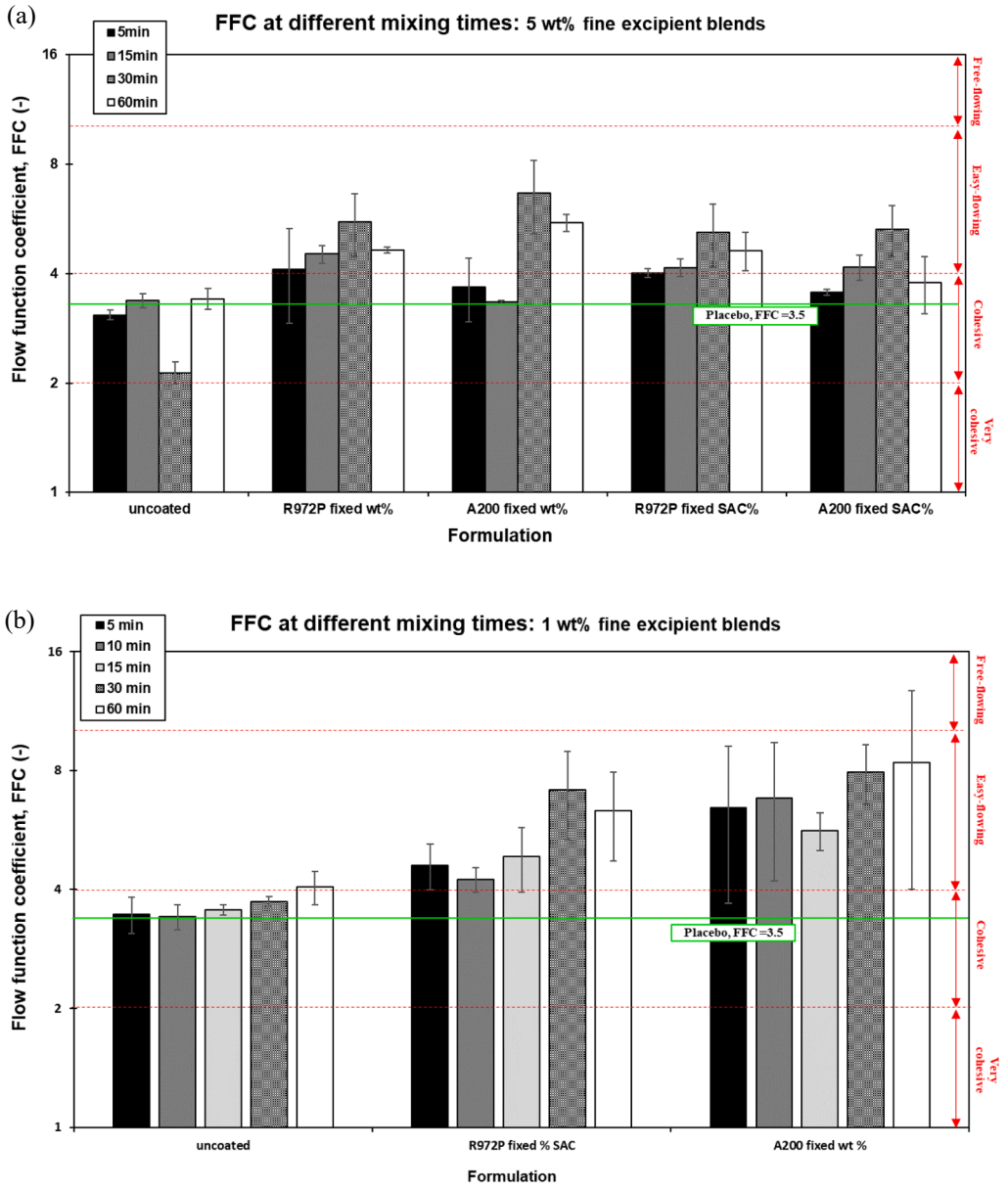


**Fig. 6.** Flowability (FFC) of low API loaded blends at different mixing times and dry coating formulations: (a) 5 wt% API loaded fine excipient blends, and (b) 1 wt% API loaded fine excipient blends. FFC values for placebos blended for 30 min denoted in bright green lines. Each measurement was repeated six times to assure reproducibility. (For interpretation of the references to colour in this figure legend, the reader is referred to the web version of this article.)

manufacturing of direct compressed tablets as well as other solid dosing forms such as capsule and sachet filling (Pitt, 2022; Tan and Newton, 1990; Sun, 2010).

As an aside, the coarse excipient blends were free flowing regardless of Ibu being dry coated or not with one exception: the 5 wt% blend with uncoated Ibu. In this case, the presence of fine powders diminished the flow to the cohesive range in contrast to the free flowing placebo of coarse excipients (the *Supplementary Material*, Fig. S3(a)), corroborating previous studies mentioning the undesirable effect of the fines on flowability of a coarse excipient blend (Hertel et al., 2018; Ma et al., 2020; Visser, 1989). Thankfully, for much lower amount of fines in the 1 wt% API loaded coarse excipient blends, the bulk flow was not adversely impacted.

### *3.3.2. Blend agglomerate size assessment: 5 wt% and 1 wt% API loadings*

As mentioned in the introduction, conventional choice of excipients with a fine cohesive API, such as Ibu25, would include a coarser class containing equal parts of Avicel PH102 and Pharmatose DCL11. However, the use of finer excipients, such as equal parts of Avicel PH105 and Pharmatose 450, led to surprising unexpected synergy that yielded a dramatic improvement in flowability of the low drug loaded blends, possibly attributed to the silica transfer and re-distribution from the surface of the API particles to the excipient particles (Chen et al., 2019; Kim et al., 2022b). A plausible question would be if the presence of silica, even though a very minute amount of the total blend, would also have an impact on the blend agglomerate size. Consequently, the examples of 5 wt% and 1 wt% blends of section 3.3.1 were analyzed at different mixing times and dry coating formulations. More interestingly, the agglomerate ratio (AR) values of all fine excipient blends of 5 wt% and 1 wt% loading cases are presented in Fig. 7(a) and 7(b), respectively. The detailed particle size distributions for primary and agglomerated size of the fine excipient blends are listed in Table 4. For the sake of brevity, the AR values for the coarse excipient blends are presented in the *Supplementary Materials*, Fig. S4 (a) S4(b), and Table S4.

(a)

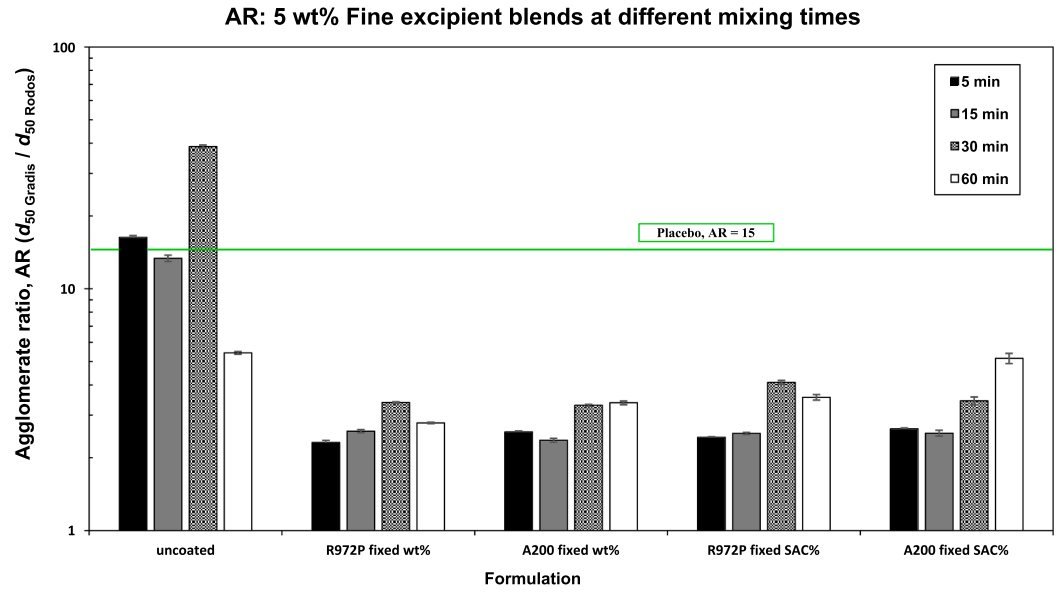


(b)

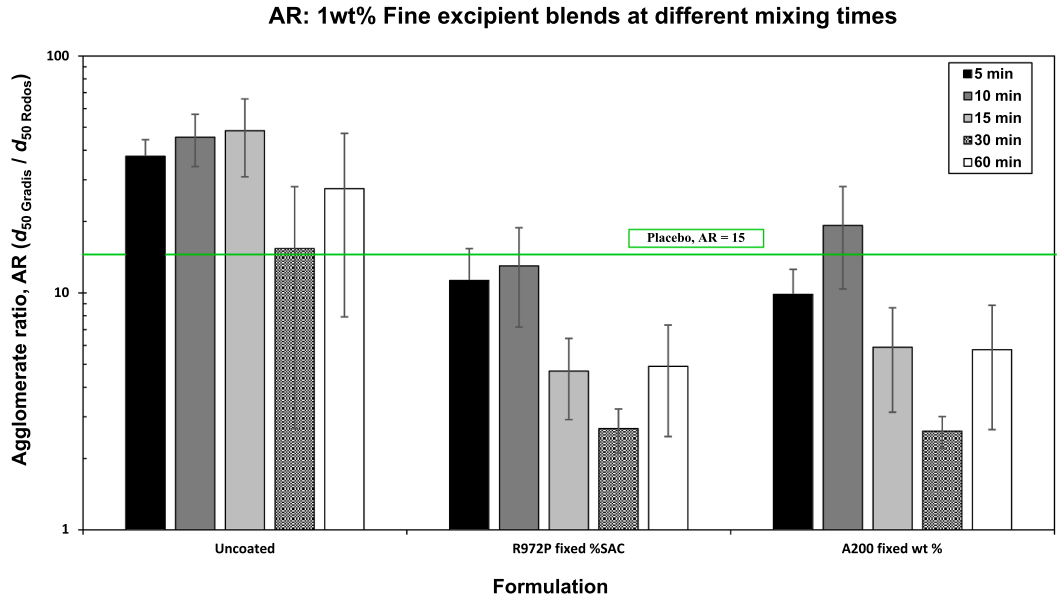


**Fig. 7.** Agglomerate ratio of low API loaded blends at different mixing times: (a) 5 wt% API loaded fine excipient blends, and (b) 1 wt% API loaded fine excipient blends.

Significant AR reduction was observed for fine excipient blends with dry coated Ibu at both drug loadings, more for 5 wt% blends, keeping in mind that the fine excipient placebo blend had an AR value of 15 (see Fig. 7(a) and 7(b) and Table 4). For 5 wt% Ibu blends, all dry coated cases achieved AR values lower than about 4 and, in some cases, even <3: An exception was the blend coated with A200 at fixed SAC for a higher mixing time of 60 min. The AR outcomes in Fig. 7(a) generally correspond with the FFC outcomes in Fig. 6(a), indicating that generally the lower the AR, the higher the FFC values. The AR values for the 1 wt% Ibu blends (Fig. 7(b)) are not as low, yet, at 30 min of mixing time, they achieved AR values below 3. Most interestingly, the FFC outcomes (Fig. 6(b)) show dramatic FFC enhancements which indicate that the extent of FFC improvements are not the same although lower AR values indicate better FFC values. Regardless, these outcomes suggest that even for blends, AR assessment could provide a preliminary indication of the flowability of the blend consisting of fine constituents.

An interesting AR trend for fine excipient blends with uncoated Ibu, was that the addition of 1 wt% fine cohesive Ibu increased AR values as compared to the placebo blend at all mixing times except for 30 min. In contrast, the 5 wt% uncoated Ibu blends had reduced the AR value with the presence of fines at the highest mixing time of 60 min, although the AR value increased at 30 min of mixing time. Overall, the FFC and AR values presented in Figs. 6 and 7 indicate that while these two properties are correlated for individual blend components, lower AR implies higher FFC (see Fig. S2, *Supplementary Materials*, also, (Kim et al., 2022a), such relationship may also exist for blends of fine powders and may warrant additional research.

A potential power-law relation between the FFC and AR of the blends was examined as shown in Fig. 8(a) and 8(b) for 5 wt% and 1 wt% loading cases, respectively. Interestingly, the trend was clearer for the 1 wt% Ibu loading. Notwithstanding the scatter observed due to different mixing times, such trend may indicate the assessment of the AR values of

**Table 4**
Selected cases of particle size distribution for 5 wt% and 1 wt% API loaded fine blends at different mixing times. Primary particle sizing was repeated at least three times, while agglomerated particle sizing was repeated at the minimum of six to eight times per sample.

| | 5 wt% loading | | | | | | | |
|---|---|---|---|---|---|---|---|---|
| Time (min) | Formulation | Agglomerate PSD, Gradis | | | | Primary PDS, Rodos (1.0 bar) | | |
| | | $d_{10}$ | $d_{50}$ | $d_{90}$ | Span$\left(\frac{d_{90}-d_{10}}{d_{50}}\right)_{Gradis}$ | $d_{10}$ | $d_{50}$ | $d_{90}$ |
| 5 | Uncoated | 24.0 ± 0.9 | 301 ± 111 | 1237 ± 543 | 4.0 | 3.3 ± 0.1 | 18.5 ± 0.1 | 46.7 ± 0.3 |
| | R972P fixed wt% | 22.7± 0.4 | 43.2 ± 1.9 | 90.3 ± 7.9 | 1.6 | 2.9 ± 0.3 | 18.7 ± 0.4 | 47.3 ± 0.2 |
| | A200 fixed wt% | 24.3± 1.3 | 47.5 ± 3.7 | 101 ± 3.3 | 1.6 | 3.6 ± 0.5 | 18.6 ± 0.1 | 47.6 ± 0.8 |
| | R972P fixed % SAC | 23.4± 0.8 | 45.6 ± 1.7 | 94.0 ± 11 | 1.6 | 3.3 ± 0.0 | 18.7 ± 0.0 | 47.5 ± 0.1 |
| | A200 fixed % SAC | 23.9± 0.8 | 48.4 ± 1.3 | 96.6 ± 8.0 | 1.5 | 3.1 ± 0.1 | 18.4 ± 0.2 | 47.1 ± 0.1 |
| 15 | Uncoated | 24.1± 1.5 | 254 ± 185 | 808 ± 415 | 3.1 | 3.0 ± 0.0 | 19.0 ± 0.1 | 56.1 ± 0.2 |
| | R972P fixed wt% | 24.0± 2.7 | 48.7 ± 4.7 | 114 ± 13 | 1.8 | 3.3 ± 0.1 | 18.9 ± 0.2 | 49.4 ± 3.0 |
| | A200 fixed wt% | 21.6± 1.3 | 45.0 ± 4.0 | 110 ± 20 | 2.0 | 3.4 ± 0.0 | 19.1 ± 0.3 | 51.8 ± 3.3 |
| | R972P fixed % SAC | 23.2± 1.0 | 47.9 ± 3.1 | 127 ± 30 | 2.2 | 3.3 ± 0.1 | 19.0 ± 0.1 | 54.4 ± 0.3 |
| | A200 fixed % SAC | 22.6± 0.6 | 47.6 ± 2.1 | 104 ± 10 | 1.7 | 3.2 ± 0.1 | 18.8 ± 0.1 | 54.5 ± 0.7 |
| 30 | Uncoated | 72.8± 68.6 | 707 ± 913 | 1683 ± 781 | 2.3 | 3.4 ± 0.1 | 18.3 ± 0.1 | 47.1 ± 0.1 |
| | R972P fixed wt% | 24.0± 2.6 | 62.1 ± 16.9 | 303 ± 158 | 4.5 | 3.5 ± 0.0 | 18.4 ± 0.0 | 47.0 ± 0.0 |
| | A200 fixed wt% | 24.0± 3.5 | 60.4 ± 22.4 | 229 ± 131 | 3.4 | 3.6 ± 0.1 | 18.3 ± 0.1 | 46.9 ± 0.2 |
| | R972P fixed % SAC | 26.4± 0.9 | 75.4 ± 10.1 | 1019 ± 708 | 13.2 | 3.6 ± 0.1 | 18.4 ± 0.1 | 47.1 ± 0.0 |
| | A200 fixed % SAC | 24.6± 10.0 | 63.3 ± 28.1 | 494 ± 364 | 7.4 | 3.6 ± 0.1 | 18.4 ± 0.1 | 47.2 ± 0.0 |
| 60 | Uncoated | 33.0± 1.3 | 104 ± 4.4 | 1194 ± 903 | 11.2 | 3.5 ± 0.1 | 19.1 ± 0.1 | 54.2 ± 0.5 |
| | R972P fixed wt% | 24.1± 1.3 | 52.4 ± 5.4 | 114 ± 19 | 1.7 | 3.1 ± 0.0 | 18.8 ± 0.0 | 54.2 ± 0.2 |
| | A200 fixed wt% | 25.0± 0.9 | 62.4 ± 7.9 | 730 ± 845 | 11.3 | 3.2 ± 0.0 | 18.5 ± 0.2 | 49.6 ± 3.2 |
| | R972P fixed % SAC | 26.2± 0.4 | 67.8 ± 9.5 | 320 ± 167 | 4.3 | 3.3 ± 0.0 | 19.1 ± 0.3 | 51.8 ± 2.9 |
| | A200 fixed % SAC | 32.9± 1.5 | 98.4 ± 8.3 | 412 ± 53 | 3.9 | 3.4 ± 0.0 | 19.1 ± 0.3 | 51.4 ± 3.3 |
| | 1 wt% loading | | | | | | | |
| Time (min) | Formulation | Agglomerate PSD, Gradis | | | | Primary PDS, Rodos (1.0bar) | | |
| | | $d_{10}$ | $d_{50}$ | $d_{90}$ | Span$\left(\frac{d_{90}-d_{10}}{d_{50}}\right)_{Gradis}$ | $d_{10}$ | $d_{50}$ | $d_{90}$ |
| 5 | Uncoated | 41.7± 2.6 | 734± 128 | 1351± 507 | 1.8 | 3.3± 0.0 | 19.5± 0.0 | 55.1± 0.5 |
| | R972P fixed % SAC | 29.9± 5.0 | 218± 75 | 730± 68 | 3.2 | 3.7± 0.0 | 19.3± 0.3 | 50.4± 3.4 |
| | A200 fixed wt% | 24.0± 2.6 | 196± 54 | 914± 208 | 4.5 | 3.9± 0.0 | 19.9± 0.0 | 55.1± 0.2 |
| 10 | Uncoated | 40.8± 12.9 | 896± 444 | 1291± 556 | 1.4 | 3.9± 0.0 | 19.7± 0.0 | 55.6± 0.4 |
| | R972P fixed % SAC | 32.3± 7.0 | 256± 110 | 652± 84 | 2.4 | 4.0± 0.0 | 19.7± 0.3 | 52.6± 3.2 |
| | A200 fixed wt% | 32.7± 6.8 | 378± 168 | 994± 117 | 2.5 | 3.9± 0.0 | 19.6± 0.3 | 52.5± 3.1 |
| 15 | Uncoated | 48.4± 7.8 | 953± 343 | 1377± 389 | 1.4 | 3.7± 0.0 | 19.7± 0.0 | 54.7± 0.3 |
| | R972P fixed % SAC | 30.1± 5.1 | 97.0± 36.3 | 370± 50 | 3.5 | 4.0±0.0 | 20.8± 0.0 | 64.0± 0.9 |
| | A200 fixed wt% | 30.8± 5.3 | 112± 52 | 429± 73 | 3.6 | 3.3± 0.0 | 18.9±0.0 | 47.8± 0.1 |
| 30 | Uncoated | 26.3± 6.1 | 294± 484 | 1180± 788 | 3.9 | 3.7± 0.1 | 19.1± 0.1 | 46.7± 0.2 |
| | R972P fixed % SAC | 22.3± 3.1 | 51.5± 10.8 | 312± 383 | 5.6 | 3.9± 0.0 | 19.3± 0.0 | 46.3± 0.3 |
| | A200 fixed wt% | 20.6± 0.8 | 50.1± 7.6 | 412± 413 | 7.8 | 3.9± 0.0 | 19.2±0.0 | 46.5± 0.2 |
| 60 | Uncoated | 28.6± 9.7 | 537± 382 | 951± 682 | 1.7 | 3.6± 0.0 | 19.5± 0.0 | 53.0±0.3 |
| | R972P fixed % SAC | 29.6± 9.0 | 96.7± 47.7 | 308± 65 | 2.9 | 3.9± 0.0 | 19.7± 0.0 | 53.3± 0.2 |
| | A200 fixed wt% | 23.0± 8.8 | 112± 120 | 276± 90 | 2.3 | 3.8± 0.0 | 19.4± 0.1 | 50.5± 0.7 |
| Primary and agglomerated PSD of the placebo blends | | | | | | | | |
| 15 | Fine excipient Placebo | 44.0±4.8 | 287±135 | 1485±916 | 5.0 | 4.7±0.3 | 19.1±0.7 | 44.7±0.6 |
| 15 | Coarse excipient Placebo | 55.6±2.2 | 131±2.5 | 235±3.9 | 1.4 | 39.3±0.2 | 114±0.3 | 223±0.7 |

the fine powder blends may provide a preliminary indication of the blend flowability. In fact, the averaged AR and FFC values of the dry coated and uncoated blends shown in Fig. 8 clearly provide evidence of such a relationship. However, it is noted that lower blend AR alone would not guarantee blend uniformity, in particular for the lowest 1 wt % Ibu loading as shown via green points for which RSD <6 % was achieved.

### 3.4. Drug release profile from tablets

The selected cases of 5 wt% blends were tested to examine impacts of dry coated material type and amount, the blend mixing time, and particle size disparity between the API and excipients on the API release rates. Two extreme cases of blend mixing times of 5 and 60 min were considered due to their expected differences in the agglomerate size span (see Table 4 and the *Supplementary Materials*, Table S4). At the drug loading of 5 wt%, sink conditions prevailed throughout the dissolution testing considering the solubility of Ibu in the dissolution buffer was 2 mg/mL (Kim et al., 2022b; Levis et al., 2003). The tablets consisting of coarse excipient blends exhibited immediate API release (well over 90 % drug released within 20 min), seen in Fig. 9(a) and 9(b), although the drug release from uncoated Ibu tablets was slightly slower at 60 min mixing time, which was expected. The API release rate was not impacted by the state of API surface coating or the mixing times for coarse excipient tablets.

In contrast, the API release rates were much slower and drastically different for the fine excipient tablets. Such difference between coarse and fine excipient tablets was not because of the tablet tensile strength and moisture content considering there were no statistically significant differences (see the *Supplementary Materials* Table S5 and Table S6). Rather, the difference in the API release profiles seem to be caused by the tablet porosity differences; the porosity was higher for coarse excipients (see Table 5). That was in line with previous papers reporting faster uptake of the dissolution medium and faster disintegration rate for tablets consisting of coarse powders (Lowenthal, 1972; Rudnic et al., 1982).

Amongst the fine excipient tablets, statistically significant differences were observed as the mixing time and the state of API surface coating were varied (the *Supplementary Materials*, Table S7). For the uncoated API fine excipient tablets, the API release rate was notably

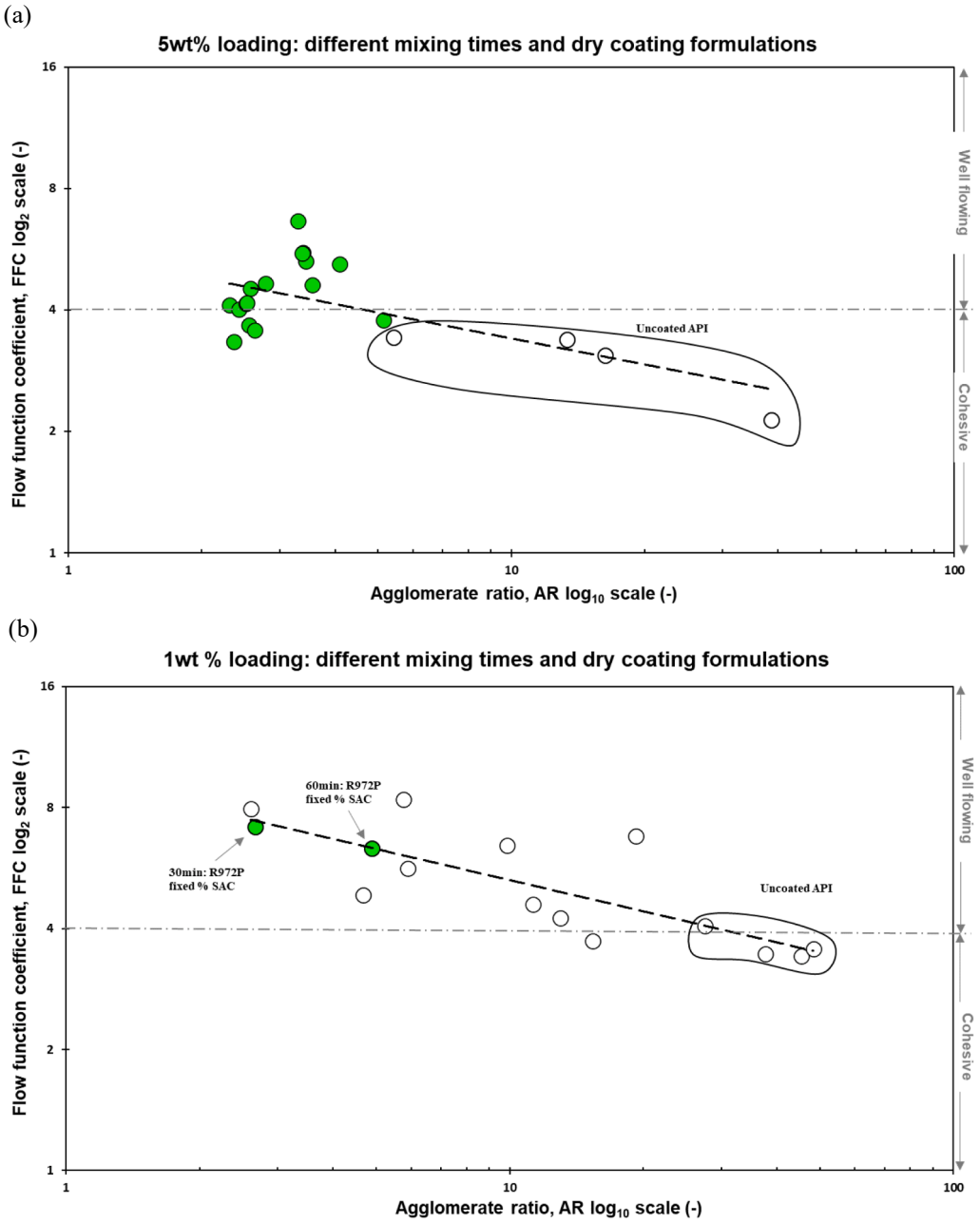


**Fig. 8.** Relationship between the agglomerate ratio (AR) of the blends and the flowability (FFC) of the blends at different mixing times and dry coating formulations: (a) 5 wt% loading cases of fine excipient blends and (b) 1 wt% loading cases of fine excipient blends. Green dots are the ones with %*RSD* lower than 6%. The dotted fitting lines for illustrative purpose. (For interpretation of the references to colour in this figure legend, the reader is referred to the web version of this article.)

improved as the mixing time was increased from 5 to 60 min. Such difference could be attributed to the blend agglomerate ratio, which is related to bulk powder cohesion (see Fig. 7(a)). To further examine the effect of mixing time, powder samples collected during the dissolution test were analyzed via optical imaging (Nikon LV100 Brightfield, Darkfield, DIC Transmitted & Reflected Light Microscope; Nikon, USA). As shown in the *Supplementary Materials*, Fig. S5(a), larger sizes and numbers of agglomerates were found in the 5-minute mixing sample. In contrast, the AR of the fine excipient blends with uncoated API went down to about 5 at 60 min mixing from the AR of over 16 at 5 min mixing (Fig. 7(a)). The similar trend was also observed in the optical image sample shown in the *Supplementary Materials* Fig. S5(a).

For the fine excipient blends with dry coated API, it was interesting to note that for 60 min mixing time, the dissolution profiles for the uncoated and dry coated API blends were statistically similar. That is expected considering the dissolution may be driven mostly by the size of excipients and resulting tablet porosity. However, at a very low mixing time of 5 min, API dry coated with hydrophobic silica R972P was much faster whereas that was not the case for hydrophilic silica A200. The reasons for such outcome are unclear considering that the disintegration times for the tablets with A200 silica coated Ibu and R972P silica coated Ibu were about the same. This was investigated further by examining powder samples collected during the dissolution test via optical imaging. As shown in the *Supplementary Materials*, Fig. S5(a) and S5(b), notable differences in the number and sizes of the visible agglomerates; a far fewer number of much smaller agglomerates were found in the R972P coated API fine excipient tablets.

In summary, dissolution from fine APIs, such as ibuprofen, is not a

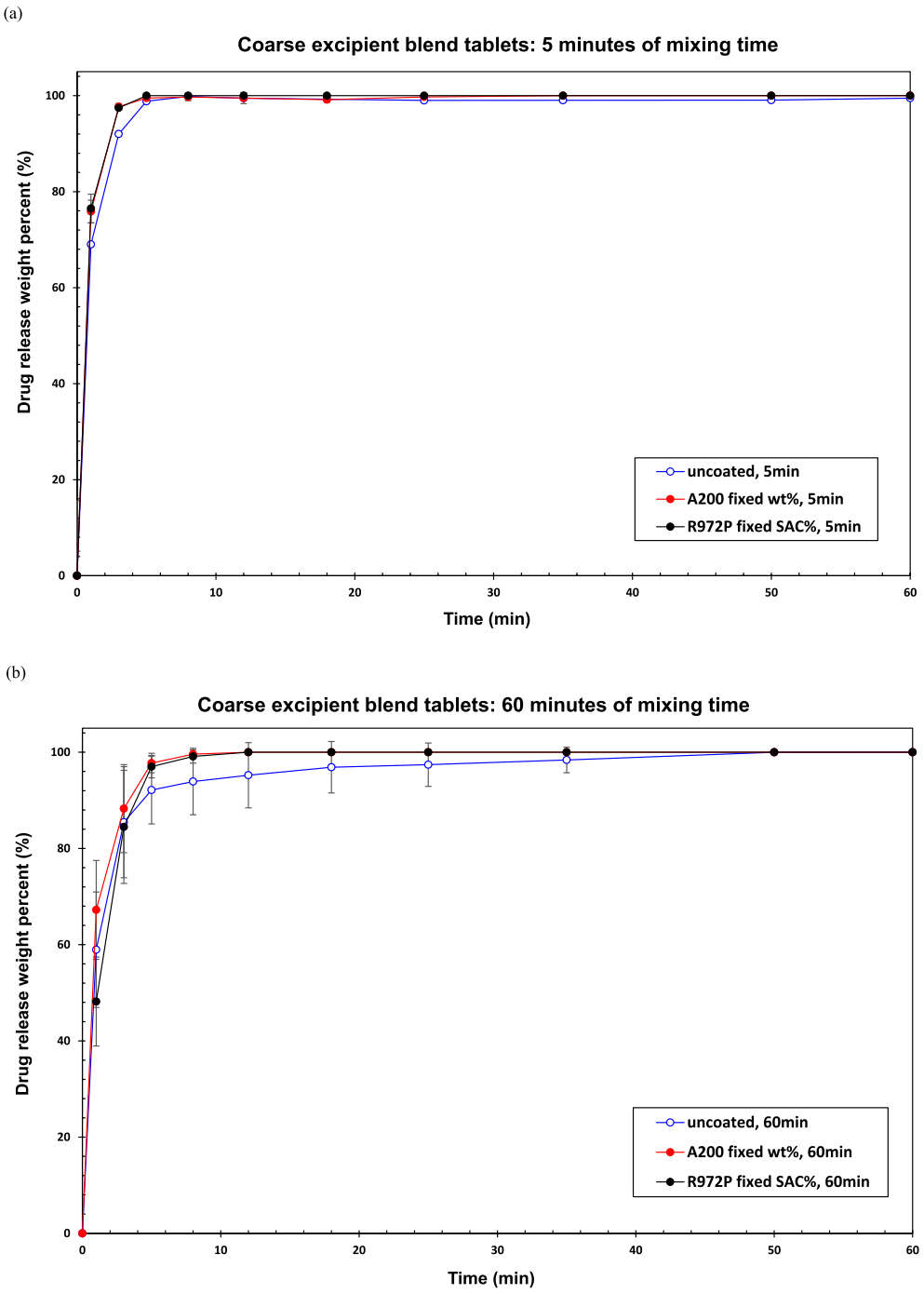


**Fig. 9.** Drug release profile for 5 wt% loaded 400 mg tablets in pH 7.2 phosphate buffer in USP II apparatus at 37.8 ± 0.3℃: (a) coarse excipient blend tablets mixing time of 5 min, (b) coarse excipient blend tablets mixing time of 60 min, (c) fine excipient blend tables mixing time of 5 min, and (d) fine excipient blend tablets mixing time of 60 min. Each test was repeated at least three times.

major concern for low drug loaded tablets consisting of larger, well flowing excipients. However, there is a concern for fine excipient tablets, considering lower tablet porosity and the ineffectiveness of excipients to break down the fine API agglomerates. Fortunately, dry coating appears to reduce the effect of mixing time and related variability without requiring a rather long mixing time, i.e., 60 min; note that the previous paper demonstrated the advantage of dry coating without having to mix for longer times (Kim et al., 2022b).

## 4. Conclusion

The assessment of the blend uniformity, flowability, and drug release rates for multi-component, low drug loaded (1, 3, and 5 wt% API), blends of fine APIs identified that the API agglomerate size, normalized as the agglomerate ratio (AR), is the main parameter governing the downstream processibility for coarse or fine excipients. Dry coating induced API agglomerate ratio reduction, as well as remarkably reduced AR of the fine excipient blends, led to enhanced blend properties, i.e., better flow and blend uniformity, suitable for precise dosing of the API.

(c)

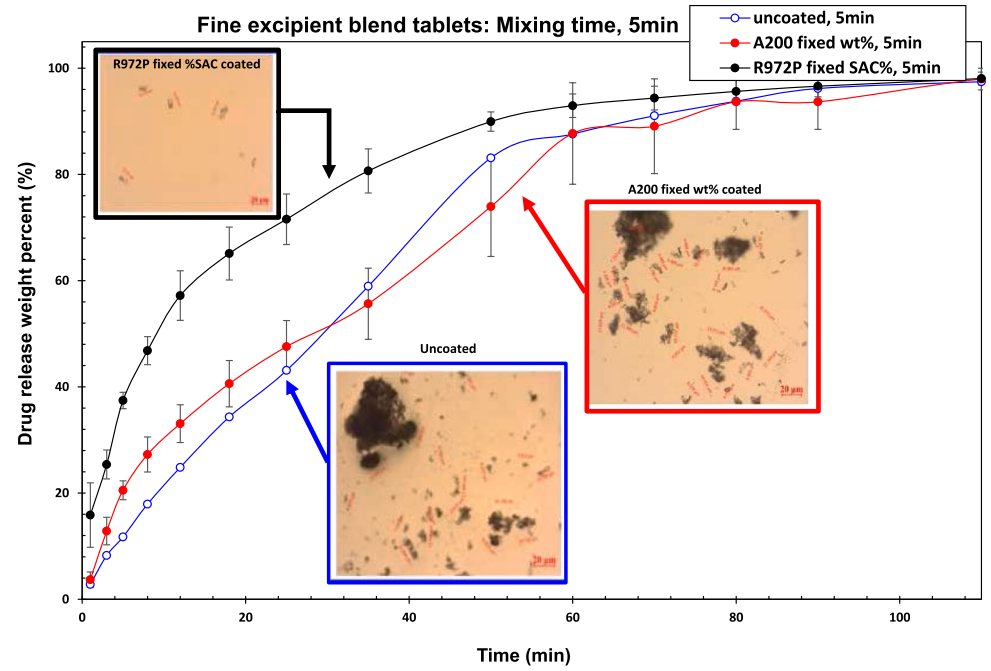


(d)

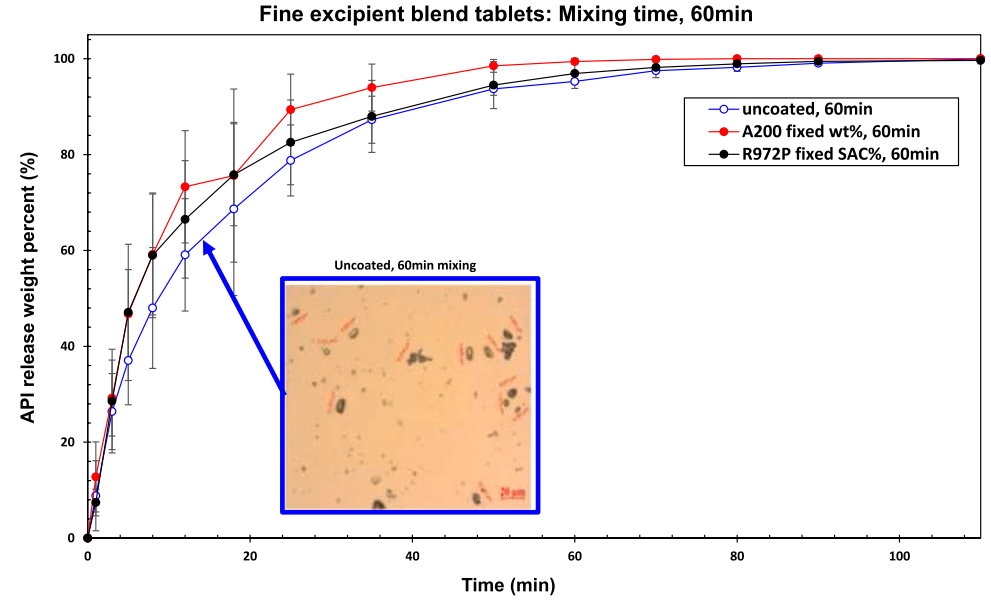


**Fig. 9.** (*continued*).

**Table 5**
Tablet porosity for those used in the dissolution assessment based on the twelve samples per formulation. Each sample was measured three times to check reproducibility.

| | Tablet Porosity | | | |
|---|---|---|---|---|
| | 5 min mixing | | 60 min mixing | |
| | Coarse | Fine | Coarse | Fine |
| Uncoated blend | 0.2313 | 0.1505 | 0.2375 | 0.1684 |
| R972P SAC% blend | 0.2495 | 0.1501 | 0.2019 | 0.1860 |
| A200 wt % blend | 0.3246 | 0.1279 | 0.2300 | 0.1926 |

In contrast, for uncoated API, the blend uniformity was poor for all blends regardless of the excipient size and mixing time. The blend properties for fine excipient blends could be further tuned by judicious selection of the dry coating formulation and mixing time. For instance, the fine excipient blends with dry coated API mixed for 30 min had enhanced flowability and lower AR. Surprisingly, the flowability was better for the lowest drug loaded blend, despite having very low amount of silica. This was most likely due to mixing induced synergy of silica redistribution. Reinforcing previous findings, dry coating led to fast API release rates even with hydrophobic silica coating and the use of fine excipients. Overall, this investigation demonstrated that for low DL blends of fine APIs, using finer excipients to minimize the particle size disparity within the blend, leads to better BU without compromising the blend flowability and dissolution rate if the API is dry coated to attain

low AR values.

*CRediT authorship contribution statement*

**Sangah S. Kim:** Conceptualization, Methodology, Validation, Formal analysis, Investigation, Data curation, Writing – original draft, Visualization, Supervision. **Chelsea Castillo:** Investigation. **Mirna Cheikhali:** Investigation. **Hadeel Darweesh:** Investigation. **Christopher Kossor:** Writing – review & editing. **Rajesh N. Davé:** Supervision, Conceptualization, Formal analysis, Data curation, Visualization, Resources, Funding acquisition, Writing – review & editing.

## Declaration of Competing Interest

The authors declare that they have no known competing financial interests or personal relationships that could have appeared to influence the work reported in this paper.

## Data availability

Data will be made available on request.

*Acknowledgements*

The authors thank Muhammed Sayedahmed and Ameera Seetahal for assistance in sample preparation and testing. The authors are grateful for stimulating discussions with and suggestions from Dr. Chen Mao, Genentech, during the CIMSEPP IAB meetings discussions. Generous donations and contributions of materials and characterization instruments are acknowledged from BASF, DFE Pharma, Evonik, Freeman Technology, FMC Biopolymer (now IFF), Gamlen, Mallinckrodt, and Surface Measurement Systems.

**Funding details**

Financial support from National Science Foundation (NSF) grants IIP- 1919037 (NSF-PFI-RP) and IIP- 2137209 (NSF-IUCRC), along with the associated Industry Advisory Board (IAB) membership support to the Center for Materials Science and Engineering of Pharmaceutical Products (CIMSEPP), is gratefully acknowledged.

## Appendix A. Supplementary material

Supplementary data to this article can be found online at https://doi.org/10.1016/j.ijpharm.2023.122722.

## References

Adi, S., Adi, H., Chan, H.K., Tong, Z., Yang, R., Yu, A., 2013. Effects of mechanical impaction on aerosol performance of particles with different surface roughness. Powder Technol. 236, 164–170.
Alexander, A., Shinbrot, T., Johnson, B., Muzzio, F.J., 2004. V-blender segregation patterns for free-flowing materials: effects of blender capacity and fill level. Int. J. Pharm. 269, 19–28.
Allenspach, C., Timmins, P., Sharif, S., Minko, T., 2020. Characterization of a novel hydroxypropyl methylcellulose (HPMC) direct compression grade excipient for pharmaceutical tablets. Int. J. Pharm. 583.
Alonso, M., 1991. title., University of Osaka Prefecture, Osaka, Japan.
Alyami, H., Dahmash, E., Bowen, J., Mohammed, A.R., 2017. An investigation into the effects of excipient particle size, blending techniques & processing parameters on the homogeneity & content uniformity of a blend containing low-dose model drug. PLoS ONE 12.
Axe, D.E., 1995. Factors affecting uniformity of a mix. Anim. Feed Sci. Technol. 53, 211–220.
Bergum, J.S., Prescott, J.K., Tejwani, R.W., Garcia, T.P., Clark, J., Brown, W., 2014. Current events in blend and content uniformity. Pharm. Eng. 34, 28–39.
Bolhuis, G.K., Smallenbroek, A.J., Lerk, C.F., 1981. Interaction of tablet disintegrants and magnesium stearate during mixing I: effect on tablet disintegration. J. Pharm. Sci. 70, 1328–1330.
Borchert, C., Sundmacher, K., 2011. Crystal aggregation in a flow tube: Image-based observation. Chem. Eng. Technol. 34, 545–556.
Bridgwater, J., 2012. Mixing of powders and granular materials by mechanical means - a perspective. Particuology 10, 397–427.
Brunaugh, A.D., Smyth, H.D.C., 2018. Formulation techniques for high dose dry powders. Int. J. Pharm. 547, 489–498.
Capece, M., Huang, Z., To, D., Aloia, M., Muchira, C., Davé, R.N., Yu, A.B., 2014. Prediction of porosity from particle scale interactions: surface modification of fine cohesive powders. Powder Technol. 254, 103–113.
Capece, M., Ho, R., Strong, J., Gao, P., 2015. Prediction of powder flow performance using a multi-component granular Bond number. Powder Technol. 286, 561–571.
Capece, M., Borchardt, C., Jayaraman, A., 2021. Improving the effectiveness of the Comil as a dry-coating process: enabling direct compaction for high drug loading formulations. Powder Technol. 379, 617–629.
Carson, J.W., Royal, T.A., Goodwill, D.J., 1986. Understanding and eliminating particle segregation problems. Bulk Solids Handl. 6, 139–144.
Castellanos, A., 2005. The relationship between attractive interparticle forces and bulk behaviour in dry and uncharged fine powders. Adv. Phys. 54, 263–376.
Chattoraj, S., Shi, L., Sun, C.C., 2011. Profoundly improving flow properties of a cohesive cellulose powder by surface coating with nano-silica through comilling. J. Pharm. Sci. 100, 4943–4952.
Chen, L., Ding, X., He, Z., Fan, S., Kunnath, K.T., Zheng, K., Davé, R.N., 2018a. Surface engineered excipients: II. Simultaneous milling and dry coating for preparation of fine-grade microcrystalline cellulose with enhanced properties. Int. J. Pharm. 546, 125–136.
Chen, L., Ding, X., He, Z., Huang, Z., Kunnath, K.T., Zheng, K., Davé, R.N., 2018b. Surface engineered excipients: I. Improved functional properties of fine grade microcrystalline cellulose. Int. J. Pharm. 536, 127–137.
Chen, L., He, Z., Kunnath, K.T., Fan, S., Wei, Y., Ding, X., Zheng, K., Davé, R.N., 2019. Surface engineered excipients: III. Facilitating direct compaction tableting of binary blends containing fine cohesive poorly-compactable APIs. Int. J. Pharm. 557, 354–365.
Chen, F.C., Liu, W.J., Zhu, W.F., Yang, L.Y., Zhang, J.W., Feng, Y., Ming, L.S., Li, Z., 2022. Surface modifiers on composite particles for direct compaction. Pharmaceutics 14.
Chen, Y., Yang, J., Dave, R.N., Pfeffer, R., 2008. Fluidization of coated group C powders. AIChE J 54, 104–121.
Dave, R.N., Chen, L., 2018. In: Dry Processed Surface Coated Engineering Excipients. Institute of Technology USA, New Jersey, p. 97.
Dave, R.N., Kim, S., Lin, Z., 2022a. Powder blend processability improvements through minimal amounts of synergistically selected surface coating agents. In: Office, U.P. (Ed.). New Jersey Institute of Technology, USA.
Dave, R.N., Kim, S., Kunnath, K., Tripathi, S., 2022b. A concise treatise on model-based enhancements of cohesive powder properties via dry particle coating. Adv. Powder Technol. 33.
Engisch, W.E., Muzzio, F.J., 2015. Loss-in-weight feeding trials case study: pharmaceutical formulation. J. Pharm. Innov. 10, 56–75.
FDA, U.S.F.D.A., 2022. Code of Federal Regulations Title 21.
Fell, J.T., Newton, J.M., 1970. Determination of tablet strength by the diametral-compression test. J. Pharm. Sci. 59, 688–691.
Freeman, R., 2007. Measuring the flow properties of consolidated, conditioned and aerated powders - a comparative study using a powder rheometer and a rotational shear cell. Powder Technol. 174, 25–33.
Fu, X., Dutt, M., Bentham, A.C., Hancock, B.C., Cameron, R.E., Elliott, J.A., 2006. Investigation of particle packing in model pharmaceutical powders using X-ray microtomography and discrete element method. Powder Technol. 167, 134–140.
Garcia, T., Bergum, J., Prescott, J., Tejwani, R., Parks, T., Clark, J., Brown, W., Muzzio, F., Patel, S., Hoiberg, C., 2015. Recommendations for the assessment of blend and content uniformity: modifications to withdrawn FDA draft stratified sampling guidance. J. Pharm. Innov. 10, 76–83.
Gera, M., Saharan, V.A., Kataria, M., Kukkar, V., 2010. Mechanical methods for dry particle coating processes and their applications in drug delivery and development. Recent Pat. Drug Deliv. Formul. 4, 58–81.
Gordon, M.S., Rudraraju, V.S., Dani, K., Chowhan, Z.T., 1993. Effect of the mode of super disintegrant incorporation on dissolution in wet granulated tablets. J. Pharm. Sci. 82, 220–226.
Gray, J.M.N.T., Thornton, A.R., 2005. A theory for particle size segregation in shallow granular free-surface flows. Proc. Roy. Soc. A: Math. Phys. Eng. Sci. 461, 1447–1473.
Han, X., Ghoroi, C., To, D., Chen, Y., Davé, R., 2011. Simultaneous micronization and surface modification for improvement of flow and dissolution of drug particles. Int. J. Pharm. 415, 185–195.
Han, X., Ghoroi, C., Davé, R., 2013a. Dry coating of micronized API powders for improved dissolution of directly compacted tablets with high drug loading. Int. J. Pharm. 442, 74–85.
Han, X., Jallo, L., To, D., Ghoroi, C., Davé, R., 2013b. Passivation of high-surface-energy sites of milled ibuprofen crystals via dry coating for reduced cohesion and improved flowability. J. Pharm. Sci. 102, 2282–2296.
Hendrickson, W., Kooyer, R., 2000. Process for making particle-coated solid substrates, USA.
Hertel, M., Schwarz, E., Kobler, M., Hauptstein, S., Steckel, H., Scherließ, R., 2018. Powder flow analysis: a simple method to indicate the ideal amount of lactose fines in dry powder inhaler formulations. Int. J. Pharm. 535, 59–67.
Honda, H., Ono, K., Ishizak, T., Matsuno, T., Katano, M., Koishi, M., 1987. Surface modification of powders by the high speed impact treatment method. J. Soc. Powder Technol. Japan 24, 6.
Honda, H., Matsuno, T., Koishi, M., 1988. Preparation of a graphite fluoride modified-polymer microsphere by a high speed impact treatment method. J. Soc. Powder Technol. Japan 25, 5.
Honda, H., Matsuno, T., Koishi, M., 1989. The effect of powder properties on dry impact blending preparation method. J. Soc. Powder Technol. Japan 25, 5.

Huang, Z., Scicolone, J.V., Gurumuthy, L., Davé, R.N., 2015a. Flow and bulk density enhancements of pharmaceutical powders using a conical screen mill: a continuous dry coating device. Chem. Eng. Sci. 125, 209–224.
Huang, Z., Scicolone, J.V., Han, X., Davé, R.N., 2015b. Improved blend and tablet properties of fine pharmaceutical powders via dry particle coating. Int. J. Pharm. 478, 447–455.
Huang, Z., Xiong, W., Kunnath, K., Bhaumik, S., Davé, R.N., 2017. Improving blend content uniformity via dry particle coating of micronized drug powders. Eur. J. Pharm. Sci. 104, 344–355.
Ishizaka, T., Ikawa, K., Kizu, N., Honda, H., Koishi, M., Yano, K., 1988. Complexation of aspirin with potato starch and improvement of dissolution rate by dry mixing. Chem. Pharm. Bull. 36, 2562–2569.
Ishizaka, T., Honda, H., Koishi, M., 1993. Drug dissolution from indomethacin-starch hybrid powders prepared by the dry impact blending method. J. Pharm. Pharmacol. 45, 4.
Iwasaki, T., 2011. Evaluation of mechanical energy applied to powders in dry processes and its application for design and preparation of functional particulate materials. Powder Eng. Technol. Appl. 257–310.
Jakubowska, E., Ciepluch, N., 2021. Blend segregation in tablets manufacturing and its effect on drug content uniformity—a review. Pharmaceutics 13.
Jallo, L.J., Schoenitz, M., Dreizin, E.L., Dave, R.N., Johnson, C.E., 2010. The effect of surface modification of aluminum powder on its flowability, combustion and reactivity. Powder Technol. 204, 63–70.
Jallo, L.J., Ghoroi, C., Gurumurthy, L., Patel, U., Davé, R.N., 2012. Improvement of flow and bulk density of pharmaceutical powders using surface modification. Int. J. Pharm. 423, 213–225.
Jetzer, M.W., Schneider, M., Morrical, B.D., Imanidis, G., 2018. Investigations on the mechanism of magnesium stearate to modify aerosol performance in dry powder inhaled formulations. J. Pharm. Sci. 107, 984–998.
Johnson, M.C., 1972. Particle size distribution of the active ingredient for solid dosage forms of low dosage. Pharm. Acta Helv 47, 13.
Jullien, R., Meakin, P., 1990. A mechanism for particle size segregation in three dimensions. Nature 344, 425–427.
Kaialy, W., Nokhodchi, A., 2015. Particle engineering for improved pulmonary drug delivery through dry powder inhalers. Advances and Challenges, Pulmonary Drug Delivery, pp. 171–197.
Kawashima, Y., Serigano, T., Hino, T., Yamamoto, H., Takeuchi, H., 1998. Design of inhalation dry powder of pranlukast hydrate to improve dispersibility by the surface modification with light anhydrous silicic acid (AEROSIL 200). Int. J. Pharm. 173, 243–251.
Kendall, K., 1994. Adhesion: molecules and mechanics. Science 263, 1720–1725.
Kim, S., Bilgili, E., Davé, R.N., 2021. Impact of altered hydrophobicity and reduced agglomeration on dissolution of micronized poorly water-soluble drug powders after dry coating. Int. J. Pharm. 606.
Kim, S., Cheikhali, C., Dave, R.N., 2022a. Decoding fine API agglomeration as a key indicator of powder flowability and dissolution: impact of particle engineering. Pharm. Res. 20.
Kim, S.S., Castillo, C., Sayedahmed, M., Dave, R.N., 2022b. Reduced fine API agglomeration after dry coating for enhanced blend uniformity and processability of low drug loaded blends. Pharmaceut. Res. (Accepted).
Koishi, M., Ishizaka, T., Nakajima, T., 1984. Preparation and surface properties of encapsulated powder pharmaceuticals. Appl. Biochem. Biotechnol. 10, 259–262.
Koishi, M., Honda, H., Ishizaka, T., Matsuno, T., Katano, T., Ono, K., 1987. Surface modification of powders by the high speed impact treatment method. J. Soc. Powder Technol. Japan 5.
Koskela, J., Morton, D.A.V., Stewart, P.J., Juppo, A.M., Lakio, S., 2018. The effect of mechanical dry coating with magnesium stearate on flowability and compactibility of plastically deforming microcrystalline cellulose powders. Int. J. Pharm. 537, 64–72.
Kottlan, A., Glasser, B.J., Khinast, J.G., 2023. Powder bed dynamics of a single-tablet-scale vibratory mixing process. Powder Technol. 414.
Kujawa, J., Cerneaux, S., Kujawski, W., 2014. Characterization of the surface modification process of Al2O3, TiO2 and ZrO2 powders by PFAS molecules. Colloids Surf. A Physicochem. Eng. Asp. 447, 14–22.
Kunnath, K., Huang, Z., Chen, L., Zheng, K., Davé, R., 2018. Improved properties of fine active pharmaceutical ingredient powder blends and tablets at high drug loading via dry particle coating. Int. J. Pharm. 543, 288–299.
Kunnath, K., Chen, L., Zheng, K., Davé, R.N., 2021. Assessing predictability of packing porosity and bulk density enhancements after dry coating of pharmaceutical powders. Powder Technol. 377, 709–722.
Lavielle, L., Martin, C., 1987. The role of the interface in carbon fibre-epoxy compositest. J. Adhes. 23, 45–60.
Lee, S.L., O'Connor, T.F., Yang, X., Cruz, C.N., Chatterjee, S., Madurawe, R.D., Moore, C. M.V., Yu, L.X., Woodcock, J., 2015. Modernizing pharmaceutical manufacturing: from batch to continuous production. J. Pharm. Innov. 10, 191–199.
Levis, K.A., Lane, M.E., Corrigan, O.I., 2003. Effect of buffer media composition on the solubility and effective permeability coefficient of ibuprofen. Int. J. Pharm. 253, 49–59.
Li, L., Sun, S., Parumasivam, T., Denman, J.A., Gengenbach, T., Tang, P., Mao, S., Chan, H.K., 2016. L-Leucine as an excipient against moisture on in vitro aerosolization performances of highly hygroscopic spray-dried powders. Eur. J. Pharm. Biopharm. 102, 132–141.
Liu, H., Lu, C., Patel, S.H., Zhu, L., Young, M.W., Gogos, C.G., Bonnett, P.C., 2012. Simultaneous milling, coating and coat-curing of particulates in a fluid energy mill via photo-polymerization. In: Annual Technical Conference - ANTEC, Conference Proceedings, pp. 2137–2141.
Lowenthal, W., 1972. Disintegration of tablets. J. Pharm. Sci. 61, 1695–1711.
Ma, Y., Evans, T.M., Philips, N., Cunningham, N., 2020. Numerical simulation of the effect of fine fraction on the flowability of powders in additive manufacturing. Powder Technol. 360, 608–621.
Massimilla, L., Donsì, G., 1976. Cohesive forces between particles of fluid-bed catalysts. Powder Technol. 15, 253–260.
Mehrotra, S., 2010. High potency active pharmaceutical ingredients (HPAPIs) the fastest growing market segment in the pharmaceutical industry. Chim. Oggi 28, 43–45.
Mei, R., Shang, H., Klausner, J.F., Kallman, E., 1997. A contact model for the effect of particle coating on improving the flowability of cohesive powders. Kona Powder Part. J. 15, 132–141.
Meyer, K., Zimmermann, I., 2004. Effect of glidants in binary powder mixtures. Powder Technol. 139, 40–54.
Mullarney, M.P., Beach, L.E., Davé, R.N., Langdon, B.A., Polizzi, M., Blackwood, D.O., 2011a. Applying dry powder coatings to pharmaceutical powders using a comil for improving powder flow and bulk density. Powder Technol. 212, 397–402.
Mullarney, M.P., Beach, L.E., Langdon, B.A., Polizzi, M.A., 2011b. Applying dry powder coatings: using a resonant acoustic mixer to improve powder flow and bulk density. Pharm. Technol. 35, 94–102.
Muselík, J., Franc, A., Doležel, P., Gonëc, R., Krondlová, A., Lukášová, I., 2014. Influence of process parameters on content uniformity of a low dose active pharmaceutical ingredient in a tablet formulation according to GMP. Acta Pharm. 64, 355–367.
Muzzio, F.J., Robinson, P., Wightman, C., 1997. Sampling practices in powder blending. Int. J. Pharm. 155, 153–178.
Naito, M., Hotta, T., Fukui, T., 2003. Applications of comminution techniques for the surface design of powder materials. Key Eng. Mater. 253, 275–292.
Nase, S.T., Vargas, W.L., Abatan, A.A., McCarthy, J.J., 2001. Discrete characterization tools for cohesive granular material. Powder Technol. 116, 214–223.
Neugebauer, P., Cardona, J., Besenhard, M.O., Peter, A., Gruber-Woelfler, H., Tachtatzis, C., Cleary, A., Andonovic, I., Sefcik, J., Khinast, J.G., 2018. Crystal shape modification via cycles of growth and dissolution in a tubular crystallizer. Cryst. Growth Des. 18, 12.
Ono, T., Yonemochi, E., 2020. Evaluation of the physical properties of dry surface-modified ibuprofen using a powder rheometer (FT4) and analysis of the influence of pharmaceutical additives on improvement of the powder flowability. Int. J. Pharm. 579.
Osorio, J.G., Muzzio, F.J., 2015. Evaluation of resonant acoustic mixing performance. Powder Technol. 278, 46–56.
Ottino, J.M., Khakhar, D.V., 2000. Mixing and segregation of granular materials. Annu. Rev. Fluid Mech. 32, 55–91.
Ouabbas, Y., Chamayou, A., Galet, L., Baron, M., Thomas, G., Grosseau, P., Guilhot, B., 2009. Surface modification of silica particles by dry coating: Characterization and powder ageing. Powder Technol. 190, 200–209.
Paajanen, M., Katainen, J., Raula, J., Kauppinen, E.I., Lahtinen, J., 2009. Direct evidence on reduced adhesion of Salbutamol sulphate particles due to L-leucine coating. Powder Technol. 192, 6–11.
Park, H., Ha, E.S., Kim, M.S., 2021. Surface modification strategies for high-dose dry powder inhalers. J. Pharm. Investig. 51, 635–668.
Pasha, M., Hekiem, N.L., Jia, X., Ghadiri, M., 2020. Prediction of flowability of cohesive powder mixtures at high strain rate conditions by discrete element method. Powder Technol. 372, 59–67.
Paul, S., Sun, C.C., 2017. The suitability of common compressibility equations for characterizing plasticity of diverse powders. Int. J. Pharm. 532, 124–130.
Pfeffer, R., Dave, R.N., Wei, D., Ramlakhan, M., 2001. Synthesis of engineered particulates with tailored properties using dry particle coating. Powder Technol. 117, 40–67.
Pingali, K., Mendez, R., Lewis, D., Michniak-Kohn, B., Cuitino, A., Muzzio, F., 2011. Mixing order of glidant and lubricant - influence on powder and tablet properties. Int. J. Pharm. 409, 269–277.
Pitt, K., 2022. Formulation and processing for powder sachets. In: Tovey, G.D. (Ed.), Specialised Pharmaceutical Formulation. Royal Society of Chemistry, p. 338.
Poux, M., Fayolle, P., Bertrand, J., Bridoux, D., Bousquet, J., 1991. Powder mixing: some practical rules applied to agitated systems. Powder Technol. 68, 213–234.
Powderprocess, 2017. Engineering resources for powder processing industries, Powder Mixing Engineering Guide, pp. A free online Engineering Guide to the mixing of powder, granules and more generally Bulk solids.
Qu, L., Morton, D.A.V., Zhou, Q.T., 2015a. Particle engineering Via mechanical dry coating in the design of pharmaceutical solid dosage forms. Curr. Pharm. Des. 21, 5802–5814.
Qu, L., Zhou, Q., Denman, J.A., Stewart, P.J., Hapgood, K.P., Morton, D.A.V., 2015b. Influence of coating material on the flowability and dissolution of dry-coated fine ibuprofen powders. Eur. J. Pharm. Sci. 78, 264–272.
Rohrs, B.R., Amidon, G.E., Meury, R.H., Secreast, P.J., King, H.M., Skoug, C.J., 2006. Particle size limits to meet USP content uniformity criteria for tablets and capsules. J. Pharm. Sci. 95, 1049–1059.
Rudnic, E.M., Rhodes, C.T., Welch, S., Bernardo, P., 1982. Evaluations of the mechanism of disintegrant action. Drug Dev. Ind. Pharm. 8, 87–109.
Rumpf, H., 1974. Die Wissenschaft des Agglomerierens. Chem. Ing. Tech. 46, 1.
Sacher, S., Heindl, N., Afonso Urich, J.A., Kruisz, J., Khinast, J.G., 2020. A solution for low-dose feeding in continuous pharmaceutical processes. Int. J. Pharm. 591.
Saeki, I., Kondo, K., Nagase, R., Yoshida, M., Niwa, T., 2019. Design of swellable ordered-mixed spherical drug particles (Swell-OM-spheres) using a dry powder milling and coating technique to improve dissolution behavior. J. Drug Delivery Sci. Technol. 54.
Schaber, S.D., Gerogiorgis, D.I., Ramachandran, R., Evans, J.M.B., Barton, P.I., Trout, B. L., 2011. Economic analysis of integrated continuous and batch pharmaceutical manufacturing: a case study. Ind. Eng. Chem. Res. 50, 10083–10092.

Schaller, B.E., Moroney, K.M., Castro-Dominguez, B., Cronin, P., Belen-Girona, J., Ruane, P., Croker, D.M., Walker, G.M., 2019. Systematic development of a high dosage formulation to enable direct compression of a poorly flowing API: a case study. Int. J. Pharm. 566, 615–630.
Schulze, D., Schwedes, J., Carson, J.W., 2008. Powders and bulk solids: behavior, characterization, storage and flow.
Senderak, E.T., 2009. Content uniformity acceptance limit for a validation batch suppositories, transdermal systems, and inhalations Validation batch CU RSD acceptance limit. Drug Dev. Ind. Pharm. 35, 735–737.
Senna, M., 1998. More chemistry for finer particle technology. Chem. Eng. Res. Des. 76, 767–774.
Senna, M., 1999. Atomic processes during mechanical compounding with metal hydroxides. Mater. Sci. Forum 312, 167–172.
Shah, U.V., Karde, V., Ghoroi, C., Heng, J.Y.Y., 2017. Influence of particle properties on powder bulk behaviour and processability. Int. J. Pharm. 518, 138–154.
Sharma, R., Setia, G., 2019. Mechanical dry particle coating on cohesive pharmaceutical powders for improving flowability - A review. Powder Technol. 356, 458–479.
Shenoy, P., Viau, M., Tammel, K., Innings, F., Fitzpatrick, J., Ahrné, L., 2015. Effect of powder densities, particle size and shape on mixture quality of binary food powder mixtures. Powder Technol. 272, 165–172.
Shetty, N., Cipolla, D., Park, H., Zhou, Q.T., 2020. Physical stability of dry powder inhaler formulations. Expert Opin. Drug Deliv. 17, 77–96.
Sierra-Vega, N.O., Román-Ospino, A., Scicolone, J., Muzzio, F.J., Romañach, R.J., Méndez, R., 2019. Assessment of blend uniformity in a continuous tablet manufacturing process. Int. J. Pharm. 560, 322–333.
Stavrou, A.G., Hare, C., Hassanpour, A., Wu, C.Y., 2020. Investigation of powder flowability at low stresses: influence of particle size and size distribution. Powder Technol. 364, 98–114.
Sun, C.C., 2008. Mechanism of moisture induced variations in true density and compaction properties of microcrystalline cellulose. Int. J. Pharm. 346, 93–101.
Sun, C.C., 2010. Setting the bar for powder flow properties in successful high speed tableting. Powder Technol. 201, 106–108.
Sun, W.J., Aburub, A., Sun, C.C., 2017. Particle engineering for enabling a formulation platform suitable for manufacturing low-dose tablets by direct compression. J. Pharm. Sci. 106, 1772–1777.
Suzuki, H., Shimizu, M., Kamiya, H., Ota, T., Takahashi, M., 1997. Preparation of fine mullite powders with high surface area by agglomeration control of alkoxide-derived precursor sol. Adv. Powder Technol. 8, 12.
Tan, B.M.J., Chan, L.W., Heng, P.W.S., 2016. Improving dry powder inhaler performance by surface roughening of lactose carrier particles. Pharm. Res. 33, 1923–1935.
Tan, S.B., Newton, J.M., 1990. Powder flowability as an indication of capsule filling performance. Int. J. Pharmaceut 61, 10.
Tang, P., Puri, V.M., 2004. Methods for minimizing segregation: a review. Part. Sci. Technol. 22, 321–337.
Tanno, K., 1990. Current status of the mechanofusion process for producing composite particles. Kona Powder Part. J. 8, 74–82.
Tinke, A.P., Govoreanu, R., Weuts, I., Vanhoutte, K., De Smaele, D., 2009. A review of underlying fundamentals in a wet dispersion size analysis of powders. Powder Technol. 196, 102–114.
USP-NF, 2011. <905> Uniformity of dosage units, in: FDA (Ed.), Stage 6 Harmonization. United States Pharmacopeia, p. 3.
Valverde, J.M., Castellanos, A., 2007. Compaction of fine powders: from fluidized agglomerates to primary particles. Granul. Matter 9, 19–24.
Vanarase, A.U., Järvinen, M., Paaso, J., Muzzio, F.J., 2013. Development of a methodology to estimate error in the on-line measurements of blend uniformity in a continuous powder mixing process. Powder Technol. 241, 263–271.
Visser, J., 1989. Van der Waals and other cohesive forces affecting powder fluidization. Powder Technol. 58, 1–10.
Vreeman, G., Sun, C.C., 2021. Mean yield pressure from the in-die Heckel analysis is a reliable plasticity parameter. Int. J. Pharm. X 3.
Wang, P., Zhu, L., Teng, S., Zhang, Q., Young, M.W., Gogos, C., 2009. A novel process for simultaneous milling and coating of particulates. Powder Technol. 193, 65–68.
Watano, S., Pfeffer, R., Dave, R., 2001. Method of Particle Coating, USA.
Watano, S., Imada, Y., Miyanami, K., Wu, C.Y., Dave, R.N., Pfeffer, R., Yoshida, T., 2000. Surface modification of food fiber by dry particle coating. J. Chem. Eng. Jpn. 33, 848–854.
Xu, C.C., Zhang, H., Zhu, J., 2009. Improving flowability of cohesive particles by partial coating on the surfaces. Can. J. Chem. Eng. 87, 403–414.
Yang, J., Sliva, A., Banerjee, A., Dave, R.N., Pfeffer, R., 2005. Dry particle coating for improving the flowability of cohesive powders. Powder Technol. 158, 21–33.
Yano, T., Ohsaki, S., Nakamura, H., Watano, S., 2021. Numerical study on compression processes of cohesive bimodal particles and their packing structure. Adv. Powder Technol. 32, 1362–1368.
Yokoyama, T., Urayama, K., Naito, M., Kato, M., Yokoyama, T., 1987. The angmill mechanofusion system and its applications. Kona Powder Part. J. 5, 59–68.
Yu, A.B., Feng, C.L., Zou, R.P., Yang, R.Y., 2003. On the relationship between porosity and interparticle forces. Powder Technol. 130, 70–76.
Yu, W., Hancock, B.C., 2008. Evaluation of dynamic image analysis for characterizing pharmaceutical excipient particles. Int. J. Pharm. 361, 150–157.
Zaborenko, N., Shi, Z., Corredor, C.C., Smith-Goettler, B.M., Zhang, L., Hermans, A., Neu, C.M., Alam, M.A., Cohen, M.J., Lu, X., Xiong, L., Zacour, B.M., 2019. First-principles and empirical approaches to predicting in vitro dissolution for pharmaceutical formulation and process development and for product release testing. AAPS Journal 21.
Zakhvatayeva, A., Zhong, W., Makroo, H.A., Hare, C., Wu, C.Y., 2018. An experimental study of die filling of pharmaceutical powders using a rotary die filling system. Int. J. Pharm. 553, 84–96.
Zhang, Q., Yang, J., Teng, S., Dave, R.N., Zhu, L., Wang, P., Young, M.W., Gogos, C.G., 2009. In-situ, simultaneous milling and coating of particulates with nanoparticles. Powder Technol. 196, 292–297.
Zheng, J.Y., 2008. Formulation and analytical development for low-dose oral drug products.
Zhou, Q.T., Qu, L., Larson, I., Stewart, P.J., Morton, D.A.V., 2011. Effect of mechanical dry particle coating on the improvement of powder flowability for lactose monohydrate: a model cohesive pharmaceutical powder. Powder Technol. 207, 414–421.
Zhou, Q.T., Leung, S.S.Y., Tang, P., Parumasivam, T., Loh, Z.H., Chan, H.K., 2015. Inhaled formulations and pulmonary drug delivery systems for respiratory infections. Adv. Drug Deliv. Rev. 85, 83–99.
Zhou, Y., Zhu, J., 2019. Group C+ particles: enhanced flow and fluidization of fine powders with nano-modulation. Chem. Eng. Sci. 207, 653–662.
Zhou, Y., Zhu, J., 2021. A review on fluidization of Geldart Group C powders through nanoparticle modulation. Powder Technol. 381, 698–720.
Zhu, F., Zhang, J., Yang, Z., Guo, Y., Li, H., Zhang, Y., 2005. The dispersion study of TiO2 nanoparticles surface modified through plasma polymerization. Physica E 27, 457–461.
Zijlstra, G.S., Hinrichs, W.L., de Boer, A.H., Frijlink, H.W., 2004. The role of particle engineering in relation to formulation and de-agglomeration principle in the development of a dry powder formulation for inhalation of cetrorelix. Eur. J. Pharm. Sci. 23, 139–149.
Zimmermann, I., Eber, M., Meyer, K., 2004. Nanomaterials as Flow Regulators in Dry Powders. Z. Phys. Chem. 218, 51–102.
Zuo, L., Lourenco, S.D.N., Baudet, B.A., 2019. Experimental insight into the particle morphology changes associated with landslide movement. Landslides 16, 787–798.